COMPUTING ABSOLUTE AND ESSENTIAL SPECTRA USING CONTINUATION

By

Jens D.M. Rademacher

Björn Sandstede

and

Arnd Scheel

IMA Preprint Series # 2054

(June 2005)

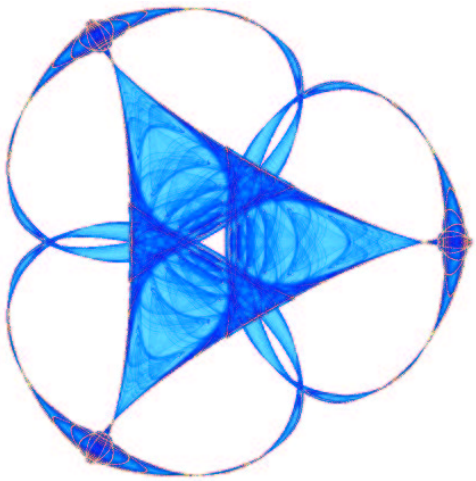

INSTITUTE FOR MATHEMATICS AND ITS APPLICATIONS

UNIVERSITY OF MINNESOTA

400 Lind Hall

207 Church Street S.E.

Minneapolis, Minnesota 55455–0436

Phone: 612/624-6066 Fax: 612/626-7370

URL: http://www.ima.umn.edu

Computing absolute and essential spectra using continuation

Jens D.M. Rademacher
Pacific Institute for the Mathematical Sciences
University of British Columbia
Vancouver, BC, V6T 1Z2, Canada

Björn Sandstede
Department of Mathematics & Statistics
University of Surrey
Guildford, GU2 7XH, UK

Arnd Scheel
School of Mathematics
University of Minnesota
Minneapolis, MN 55455, USA

June 21, 2005

Abstract

A continuation approach to the computation of essential and absolute spectra of reaction-diffusion operators on the real line is presented. The advantage of this approach compared with direct eigenvalue computations for the discretized operator are the efficient and accurate computation of selected parts of the spectrum (typically those near the imaginary axis) and the option to compute nonlinear travelling waves and selected eigenvalues, or other stability indicators, simultaneously to precisely locate the onset to instability. We also discuss the implementation and usage of this approach with the software package AUTO, and provide example computations for the FitzHugh–Nagumo and the complex Ginzburg–Landau equation.

1 Introduction

The goal of this paper is to present a consistent path-following approach for the computation of absolute and essential spectra of waves on one-dimensional domains. The eigenvalue problems that we are specifically interested in arise when linearizing nonlinear evolution equations about nonlinear waves. As a paradigm, we consider reaction-diffusion systems

$$u_t = Du_{xx} + cu_x + f(u), \qquad x \in \mathbb{R} \tag{1.1}$$

where $u \in \mathbb{R}^N$ and f is smooth. To make (1.1) well-posed, we shall assume throughout this paper that D is a positive diagonal matrix. Suppose now that $u_*(x)$ is a stationary solution of (1.1) so that

$$|u_*(x) - u_\pm(x)| \to 0 \qquad \text{as } x \to \pm\infty$$

where the asymptotic states $u_\pm(x)$ are constant or periodic in x. A natural question then is whether the equilibrium $u_*(x)$ is stable as a solution to the nonlinear evolution problem (1.1). Insight into this issue can be gained by analysing the spectrum of the linear operator

$$\mathcal{L}_* = D\partial_{xx} + c\partial_x + f_u(u_*(x)) \tag{1.2}$$

which arises when (1.1) is linearized about u_*.

The spectrum of the operator (1.2) on $L^2(\mathbb{R}, \mathbb{C}^N)$ is the disjoint union of the *essential spectrum* $\Sigma_{\rm ess}$ and the *point spectrum* $\Sigma_{\rm pt}$ which consists by definition of all isolated eigenvalues with finite multiplicity (and is therefore discrete). While the point spectrum involves the full nonlinear wave u_*, the boundary of the essential spectrum is entirely determined by the linearization of (1.1) about the asymptotic states $u_\pm$ [4, Appendix to §5].

Also of interest are finite but large domains of the form $(-\ell, \ell)$ with $\ell \gg 1$. When considering (1.2) on $(-\ell, \ell)$, we add appropriate linear separated boundary conditions of the form

$$Q_\pm^{\rm bc} \begin{pmatrix} u(\pm\ell) \\ u_x(\pm\ell) \end{pmatrix} = 0, \qquad Q_\pm^{\rm bc} \in \mathbb{R}^{2N\times 2N}, \qquad \operatorname{rank} Q_\pm^{\rm bc} = N \tag{1.3}$$

at $x = \pm\ell$. While the spectrum Σ_ℓ of the operator $\mathcal{L}_*$ on $(-\ell, \ell)$ is then necessarily discrete for each finite ℓ, we can still distinguish different parts in the limit $\ell \to \infty$ [9]: Generically, the set Σ_ℓ converges in the symmetric Hausdorff distance to a limiting set Σ_∞ which again consists of a discrete and a continuous part. The discrete part is the union of the *extended point spectrum* $\Sigma_{\rm ext}$, which contains in particular the point spectrum $\Sigma_{\rm pt}$ of the profile $u_*(x)$ on $\mathbb{R}$, and the *boundary spectrum* $\Sigma_{\rm bc}$, which is generated by the boundary conditions (1.3). The continuous part is called the *absolute spectrum* which, in general, differs from the essential spectrum. As $\ell \to \infty$, each element of the absolute spectrum is approached by infinitely many eigenvalues of $\mathcal{L}_*$ which therefore cluster near the absolute spectrum. As already alluded to, the discrete part depends on the full profile u_* and on the specific boundary conditions employed. The absolute spectrum, however, depends again only on the asymptotic states $u_\pm$, but not on the boundary conditions (as long as they are separated) or the profile u_* [10].

The absolute spectrum of spatially periodic waves is also relevant for the spectra of spiral waves on large disks [8], and it plays an important role when the nonlinear wave u_* on $\mathbb{R}$ contains long plateaus where it is close to another rest state or a periodic wave [11]. Lastly, we remark that the wave u_* typically persists on $(-\ell, \ell)$ under boundary conditions of the form (1.3). If we denote the resulting family of waves by $u_*^\ell(x)$ so that $u_*^\ell(x) \to u_*(x)$ on compact subsets of $\mathbb{R}$, then the statements made above are still true if we replace $\mathcal{L}_*$ by the linearization of (1.1) about u_*^ℓ provided the convergence is rapid enough.

In summary, the continuous parts of the spectrum ℓ_* on $\mathbb{R}$ or $(-\ell, \ell)$ are entirely determined by the asymptotic states $u_\pm$ which, we assumed, are constant or periodic in x. We shall therefore from now on focus entirely on operators with constant or periodic coefficients.

The aim of this paper is to outline reliable and efficient ways to compute these spectra using cheap but accurate continuation algorithms *without* solving discretized matrix eigenvalue problems. For the convenience of the reader, we describe in some detail how our strategies can be implemented in the boundary-value solver AUTO [2]. We will also mention various extensions to the computation of linear spreading speeds and linear instability thresholds such as Eckhaus boundaries.

As a general rule, the methods presented here can be adapted easily to dispersive equations such as members of the Korteweg–de Vries family or coupled nonlinear Schrödinger equations. Some of our arguments can also be adapted to periodic structures in higher space dimensions via Fourier and Bloch wave decomposition. We remark, however, that absolute spectra have not been used so far for genuinely higher-dimensional problems.

2 Notation and hypotheses

We consider the operator

$$\mathcal{L} := D\partial_{xx} + c\partial_x + a(x) \tag{2.1}$$

where we shall always assume that the entries d_j of the diagonal matrix $D = \mathrm{diag}(d_j)$ are strictly positive for all j and that the coefficient matrix $a(x)$ is constant or periodic in x:

Hypothesis (C) *The coefficients $a(x) = a_0 \in \mathbb{R}^{N\times N}$ do not depend on x.*

Hypothesis (P) *The coefficients $a(x) \in C^1(\mathbb{R}, \mathbb{R}^{N\times N})$ are periodic in x with minimal period $L > 0$.*

The eigenvalue problem

$$\mathcal{L}u = Du_{xx} + cu_x + a(x)u = \lambda u \tag{2.2}$$

can then also be written as

$$\begin{aligned} u_x &= v \\ v_x &= D^{-1}[\lambda u - cv - a(x)u] \end{aligned} \tag{2.3}$$

or equivalently as

$$U_x = [A(x) + \lambda B]U \tag{2.4}$$

where $U = (u, v) \in \mathbb{C}^{2N}$ and

$$A(x) = \begin{pmatrix} 0 & 1 \\ -D^{-1}a(x) & -cD^{-1} \end{pmatrix}, \qquad B = \begin{pmatrix} 0 & 0 \\ D^{-1} & 0 \end{pmatrix}.$$

Solutions to the eigenvalue problem (2.2) are therefore found by solving the initial value problem (2.3). For periodic coefficients, we denote by

$$\Phi_\lambda : \quad \mathbb{C}^{2N} \longrightarrow \mathbb{C}^{2N}, \quad (u_0, v_0) \longmapsto \Phi_\lambda(u_0, v_0) := (u, v)(L) \tag{2.5}$$

the linear time-L map of (2.3) that associates to each initial condition (u_0, v_0) the solution of (2.3) at time L. We refer to the eigenvalues of Φ_λ as spatial Floquet multipliers and to their logarithms as spatial Floquet exponents.

Note that nonlinear periodic waves can be found as periodic solutions of the first-order system

$$U_x = F(U, c), \qquad U = \begin{pmatrix} u \\ v \end{pmatrix} \in \mathbb{R}^{2N}, \qquad F(U, c) = \begin{pmatrix} v \\ -D^{-1}f(u, c) + cv \end{pmatrix}. \tag{2.6}$$

If $u_*(x)$ denotes a constant or periodic solution of (2.6), then $a(x) = f_u(u_*(x))$ in (2.2).

Most of the results presented here do not require $d_j > 0$. In this case, however, we need that the speed c does not vanish. If a concrete model has $d_j = 0$ for one or more indices j, we may also set $d_j = \delta$ for sufficiently small $\delta > 0$. The result of [6, Chapter 3.2] shows that the resulting spectra are continuous in δ on any bounded subset of the complex plane $\mathbb{C}$ as $\delta \to 0$.

3 Essential spectra

3.1 Characterizing essential spectra via Bloch waves

For constant coefficients $a(x) \equiv a_0$, we consider the Fourier transformed operator

$$\mathcal{L}_\nu := D\nu^2 + c\nu + a_0 : \quad \mathbb{C}^N \to \mathbb{C}^N \tag{3.1}$$

for $\nu \in \mathbb{C}$. Using that the Fourier transform is an isomorphism on L^2 which turns $\mathcal{L}$ into a multiplication operator, we immediately obtain the following lemma.

Lemma 3.1 *For constant coefficients, we have*

$$\operatorname{spec}\mathcal{L} = \cup_{\nu\in \mathrm{i}\mathbb{R}} \operatorname{spec}\mathcal{L}_\nu.$$

In particular, the following assertions are equivalent:

(i) $\lambda \in \operatorname{spec}\mathcal{L}$,

(ii) $[D\nu^2 + c\nu + a_0 - \lambda]u = 0$ *for some* $u \in \mathbb{C}^N$ *with* $u \neq 0$ *and some* $\nu \in \mathrm{i}\mathbb{R}$,

(iii) $d(\lambda,\nu) := \det(D\nu^2 + c\nu + a_0 - \lambda) = 0$ *for some* $\nu \in \mathrm{i}\mathbb{R}$.

While the third condition gives the most compact criterion, the second condition is, in general, preferable for numerical computations.

Note that the spectrum of the matrix $\mathcal{L}_\nu$ consists for each ν of precisely N temporal eigenvalues λ_j, counted with multiplicity. Furthermore, the eigenvalues λ_j can be continued globally in γ since they are roots of the complex analytic equation $d(\lambda,\nu) = 0$. In fact, we easily obtain:

Lemma 3.2 *The essential spectrum of* $\mathcal{L}$ *is the union of at most* N *connected components, each containing an eigenvalue* λ_j *of the linearized reaction kinetics* a_0 *and the point at infinity. Furthermore, we have* $|\arg\lambda| \to \pi$ *as* $|\gamma| \to \infty$ *in each connected component of the essential spectrum.*

We remark that it is not difficult to derive expansions for the location of the curves as $|\gamma| \to \infty$.

For periodic coefficients $a(x)$, there is a similar characterization. For each $\nu \in \mathbb{C}$, we define the Bloch-wave operator

$$\mathcal{L}_\nu := D(\partial_x + \nu)^2 + c(\partial_x + \nu) + a(x) \tag{3.2}$$

which is closed and densely defined on $L^2(0,L)$ with periodic boundary conditions $u(0) = u(L)$ and $u_x(0) = u_x(L)$.

Lemma 3.3 *For periodic coefficients with minimal period* $L > 0$, *we have*

$$\operatorname{spec}\mathcal{L} = \cup_{\nu\in \mathrm{i}[0,2\pi/L)} \operatorname{spec}\mathcal{L}_\nu.$$

In particular, the following assertions are equivalent:

(i) $\lambda \in \operatorname{spec}\mathcal{L}$,

(ii) $[D(\partial_x + \nu)^2 + c(\partial_x + \nu) + a(x) - \lambda]u = 0$ *for some* $u \in H^2_{\mathrm{per}}(0,L)$ *and some* $\nu \in \mathrm{i}\mathbb{R}$,

(iii) $d(\lambda,\nu) := \det(\Phi_\lambda - \mathrm{e}^{\nu L}) = 0$ *for some* $\nu \in \mathrm{i}[0, 2\pi/L)$.

The proof is a consequence of the Bloch-wave decomposition $L^2(\mathbb{R}) \cong \oplus_{\nu\in \mathrm{i}[0,2\pi/L)} L^2(0,L)$ given by the isomorphism

$$u(x) = \int_{\nu\in \mathrm{i}[0,2\pi/L)} \mathrm{e}^{\nu x} u(x;\nu)\,\mathrm{d}\nu,$$

where $u \in L^2(\mathbb{R})$ and $u(x;\nu) = u(x+L;\nu)$ [12]. Since the direct computation of the Floquet exponents ν of the period map Φ_λ of the ODE is often numerically unstable, condition (ii) is again preferable, from a numerical viewpoint, to the seemingly simpler condition (iii).

The operators $\mathcal{L}_\nu$ have compact resolvent for each ν, and their spectra consist therefore of isolated eigenvalues with finite multiplicity whose real parts accumulate at $-\infty$. In particular, we denote the countably many

eigenvalues of $\mathcal{L}_0$ by λ_j, which we order so that their real parts decrease as j increases. The roots λ_j of the complex analytic dispersion relation $d(\lambda,\nu)$ can again be continued globally in $\nu = \mathrm{i}\gamma$. In particular, it suffices to solve for $\gamma \in [0, 2\pi/L)$ since we then have necessarily $\lambda_j(2\pi\mathrm{i}/L) = \lambda_{\Pi(j)}(0)$ for some permutation Π of $\mathbb{N}$.

Lemma 3.4 *For periodic coefficients, the essential spectrum of $\mathcal{L}$ is an at most countable union of connected sets, each of which contains a point in the spectrum of $\mathcal{L}_0$, that is, an eigenvalue of the operator considered on $(0, L)$ with periodic boundary conditions.*

Note that the connected components do not need to contain a point at infinity. Isolas are possible, and the spectrum may not be connected on the Riemann sphere $\bar{\mathbb{C}}$, see §4.3 and §5.2.

Lastly, we briefly comment on the effect of coordinate transformations of the form $x \mapsto x - c_* t$ which correspond to changing the frame of reference in which spectra are computed. For constant coefficients, the passage to a comoving frame $\xi = x - c_* t$ simply introduces an additional drift term $c_* u_\xi$ in the expression for $\mathcal{L}$. Thus, the eigenvalues Λ in the frame ξ can be computed from solutions $\lambda(\nu)$ of $d(\lambda,\nu) = 0$ via $\Lambda = \lambda(\nu) - c_*\nu$. A similar result is true for periodic coefficients though the equation becomes time-dependent, and we therefore have to consider the period map Ψ_T of the linear PDE

$$u_t = D u_{\xi\xi} + (c + c_*) u_\xi + a(\xi + c_* t) u$$

with $T = L/c_*$.

Proposition 3.5 ([10]) *The essential spectrum of Ψ_T is of the form $\rho = \mathrm{e}^{\Lambda T}$ where $\Lambda = \lambda(\nu) - c_*\nu$, and $\lambda(\nu)$, with $\nu = \mathrm{i}\gamma$ with $\gamma \in [0, 2\pi/L)$, satisfies $d(\lambda(\nu), \nu) = 0$.*

Thus, the computation of spectra in an arbitrary frame reduces to the solution of an eigenvalue problem of the type as considered above. Note that spectral stability does not depend on the frame since the real part of the spectrum is independent of the coordinate frame by Proposition 3.5.

3.2 A priori estimates

For both (C) and (P), a straightforward scaling result shows that for each fixed $\delta \in (0, \frac{\pi}{2})$ there is a constant $R > 0$ so that $\mathcal{L}$ does not have any spectrum with $|\lambda| > R$ and $|\arg\lambda| < \frac{\pi}{2} + \delta$.

It will also turn out to be useful to consider the dispersion relations $d(\lambda,\nu)$ for purely imaginary temporal and spatial eigenvalues so that $\lambda = \mathrm{i}\omega$ and $\nu = \mathrm{i}\gamma$ for $\omega, \gamma \in \mathbb{R}$. We prove here that all real roots (ω,γ) of $d(\mathrm{i}\omega, \mathrm{i}\gamma)$ lie in bounded rectangles of $\mathbb{R}^2$ and provide estimates for these squares.

For constant coefficients, we assert (and refer to [6, Lemma 10] for the proof using Gershgorin circles) that any real solution (ω,γ) of $d(\mathrm{i}\omega, \mathrm{i}\gamma) = 0$ satisfies

$$(\omega,\gamma) \in [-|c|R_0, |c|R_0] \times [-R_0, R_0]$$

where

$$R_0^2 = \max_{j=1,\dots,N} \frac{1}{d_j} \left(a_{jj} + \sum_{i=1, i\neq j}^{N} |a_{ij}| \right).$$

For periodic coefficients, we write $\mathcal{L}$ as the sum of the diagonal constant-coefficients operator $\mathcal{L}^0$

$$\mathcal{L}^0 = \mathrm{diag}(d_j)\partial_{xx} + c\partial_x + \mathrm{diag}(\overline{a}_{jj}),$$

where $\overline{a} = \int a(x)\,\mathrm{d}x$, and the bounded remainder $\mathcal{L}^1$ which can be estimated in the operator norm on $L^2(\mathbb{R}, \mathbb{R}^N)$ by

$$\|\mathcal{L}^1\| \leq \sup_{x\in\mathbb{R}} |a(x) - \operatorname{diag}(\overline{a}_{jj})|,$$

where the norm on the right-hand side is the matrix norm induced by the norm used on $\mathbb{R}^N$ (the Euclidean norm on $\mathbb{R}^N$, for instance, induces the matrix norm $|A| = \sqrt{\sigma(A^T A)}$ where $\sigma(B)$ denotes the spectral radius of the matrix B). Using the explicit resolvent estimate

$$\|(\lambda - \mathcal{L}^0)^{-1}\| \leq \sup\{|-d_j k^2 + c\mathrm{i}k + \overline{a}_{jj} - \lambda|^{-1};\ j = 1, \ldots, N,\ k \in \mathbb{R}\},$$

we see that the spectrum of $\mathcal{L}$ is contained in an $\|\mathcal{L}^1\|$-neighborhood of the spectrum

$$\operatorname{spec}\mathcal{L}^0 = \{-d_j k^2 + c\mathrm{i}k + \overline{a}_{jj};\ j = 1, \ldots, N,\ k \in \mathbb{R}\}$$

of $\mathcal{L}^0$. Thus, any real root (ω, γ) of $d(\mathrm{i}\omega, \mathrm{i}\gamma)$ satisfies

$$(\omega, \gamma) \in [-|c|R_1, |c|R_1] \times [-R_1, R_1]$$

where

$$R_1^2 = \max_{j=1,\ldots,N} \frac{1}{d_j}\left[\overline{a}_{jj} + \|\mathcal{L}^1\|\right] \leq \max_{j=1,\ldots,N} \frac{1}{d_j}\left[\overline{a}_{jj} + \sup_{x\in\mathbb{R}} |a(x) - \operatorname{diag}(\overline{a}_{kk})|\right].$$

A rough estimate for the real parts therefore is

$$\operatorname{Re}\operatorname{spec}(\mathcal{L}) \leq \max_{j=1,\ldots,N} \bar{a}_{jj} + \sup_{x\in\mathbb{R}} |a(x) - \operatorname{diag}(\bar{a}_{kk})|.$$

3.3 Constant coefficients

3.3.1 Computing essential spectra using continuation

For constant coefficients, we had seen that we can compute the essential spectrum of $\mathcal{L}$ by continuing the N temporal eigenvalues λ of the matrix $\mathcal{L}_\nu$ defined in (3.1) in the parameter $\nu = \mathrm{i}\gamma$. Thus, starting from $\nu = 0$, say, where the temporal eigenvalues appear as eigenvalues of the matrix a_0, we can use the complex normalized eigenvalue equation

$$[-D\gamma^2 + c\mathrm{i}\gamma + a_0 - \lambda]u = 0, \qquad \langle u_{\mathrm{old}}, u\rangle = 1, \tag{3.3}$$

where u_{old} denotes the eigenvector from a previous infinitesimal step in the continuation parameter γ or the initially supplied solution at the beginning of the continuation. The condition

$$\langle u_{\mathrm{old}}, u\rangle = 1 \tag{3.4}$$

is evaluated in the complex plane and therefore fixes the norm of the solution u and its complex phase. Such a condition is necessary as solutions to

$$[-D\gamma^2 + c\mathrm{i}\gamma + a_0 - \lambda]u = 0$$

are, of course, not unique but come in group orbits $\{r\mathrm{e}^{\mathrm{i}\alpha}u;\ \alpha, r \in \mathbb{R}\}$. Equation (3.4) can be replaced by any other condition that fixes a unique element in the group orbit of solutions. Bordering conditions similar to (3.4) will occur throughout this paper to enforce uniqueness of solutions.

3.3.2 Testing stability

Often, the spectrum is only computed to check whether a given homogeneous equilibrium is stable (i.e. whether its essential spectrum lies completely in the open left-half plane). For $N = 2$, the spectrum is strictly stable if, and only if,

(i) $\det(a_0) > 0$ and $\operatorname{tr}(a_0) < 0$, and

(ii) $a^0_{22}d_1 + a^0_{11}d_2 < 0$ or $(d_1a^0_{22} - d_2a^0_{11})^2 + 4d_1d_2a^0_{12}a^0_{21} < 0$

where $a_0 = (a^0_{ij})$ (see e.g. the computations in [1]). For general N, connectedness of the essential spectrum on the Riemann sphere as stated in Lemma 3.2 immediately gives the following stability criterion.

Lemma 3.6 *The essential spectrum of $\mathcal{L}$ is contained in the open left-half plane if, and only if, it does not intersect the imaginary axis.*

Remark 3.7 *When some of the diffusion coefficients d_j vanish, then the conclusion of the lemma remains true provided $c \neq 0$ and all eigenvalues λ_j of a_0 lie in the open left half-plane.*

To determine whether the essential spectrum intersects the imaginary axis, we do not need to calculate the entire essential spectrum. It suffices to compute the $2N$ spatial eigenvalues ν for $\lambda \in \mathrm{i}\mathbb{R}$ through continuation in λ. The above lemma then states that the equilibrium is stable provided $\operatorname{Re}\nu_j \neq 0$ for all $\lambda \in \mathrm{i}\mathbb{R}$ and each $1, \dots, 2N$. A strategy for determining stability therefore goes as follows:

(i) Compute the $2N$ solutions $\nu_j(0)$ of $d(0, \nu) = 0$ and find the associated nontrivial solutions u_j of the equation
$$[D\nu^2 + c\nu + a_0]u = 0, \qquad |u| = 1.$$

(ii) Follow each (ν_j, u_j) as solutions to
$$[D\nu^2 + c\nu + a_0 - \mathrm{i}\omega]u = 0, \qquad \langle u_{\mathrm{old}}, u\rangle = 1 \tag{3.5}$$
by continuation in $\omega \in [0, |c|R_0]$ with R_0 as in §3.2, starting at $\omega = 0$.

(iii) Stability is equivalent to $\operatorname{Re}\nu_j(\mathrm{i}\omega) \neq 0$ for all $\omega \in [0, |c|R_0]$.

3.3.3 Generic singularities

When continuing roots λ or ν of $d(\lambda, \nu) = 0$ in the real parameters $\nu = \mathrm{i}\gamma$ or $\lambda = \mathrm{i}\omega$, it is of interest to know what the generic singularities are that one may encounter. On the level of the dispersion relation, this question can be easily answered.

Continuation of λ in $\nu = \mathrm{i}\gamma$: We can always continue eigenvalues λ as functions of $\nu = \mathrm{i}\gamma$ by the implicit function theorem unless $\partial_\lambda d(\lambda, \nu) = 0$. Thus, suppose, without loss of generality, that $\partial_\lambda d(\lambda, \nu) = 0$ at $\lambda = \nu = 0$ so that
$$d(\lambda, \nu) = \alpha_2\lambda^2 + \beta_1\nu + \mathrm{O}(|\nu|^2 + |\lambda\nu| + |\lambda|^3).$$
If $\alpha_2\beta_1 \neq 0$, then the Newton polygon shows that the solution set in $\nu = \mathrm{i}\gamma$ is given locally by the curves
$$\lambda(\mathrm{i}\gamma) = \pm\mathrm{i}\sqrt{\beta_1/\alpha_2}\sqrt{\gamma} + \mathrm{O}(|\gamma|) \tag{3.6}$$

for $\gamma \in \mathbb{R}$ close to zero. The coefficients α_2 and β_1 are real whenever the singularity occurs for real λ.

Due to analyticity, the equations $d = 0$ and $\partial_\lambda d = 0$ can be satisfied together either only at a discrete number of points (λ, ν) or else along curves. In the latter case, at least two branches of the essential spectrum coincide and d, $\partial_\lambda d$ have a common factor by Bézout's theorem. This is, for instance, excluded if the diffusion rates are pairwise different [6, Lemma 10]. Otherwise, the number of isolated double roots, counted with multiplicity, is equal to the degree of the resultant of $d(\cdot, \nu)$ and $\partial_\lambda d(\cdot, \nu)$ which is at most $2N(2N-1)$. In particular, we expect that we do not encounter any singularities during continuation in $\nu = \mathrm{i}\gamma$ since they should not occur for purely imaginary ν. Thus, generically, we are able to continue temporal eigenvalues in the real parameter γ in a smooth fashion. An exception is the reversible situation $c = 0$ where the dispersion relation depends analytically on $\nu^2 = -\gamma^2$, so temporal eigenvalues can collide on the real axis and split into complex conjugate pairs.

Continuation of ν in $\lambda = \mathrm{i}\omega$: To determine stability, we proposed to continue the $2N$ roots ν_j as functions of $\lambda = \mathrm{i}\omega$, whose singularities are of the form

$$d(\lambda, \nu) = \alpha_1 \lambda + \beta_2 \nu^2 + \mathrm{O}(|\nu|^3 + |\lambda\nu| + |\lambda|^2).$$

If d and $\partial_\nu d$ have no common factors, the number of double roots is again finite and, in fact, not larger than $N(2N-1)$ by Lemma 4.5 below. The roots ν unfold in the same way as the roots λ in (3.6) above. Since these singularities occur for discrete values of λ, they do typically not occur during continuation in $\lambda = \mathrm{i}\omega$.

3.4 Periodic coefficients

3.4.1 Continuation-based computation of the essential spectrum

For periodic coefficients, we can compute the essential spectrum of $\mathcal{L}$ by continuing the countably many temporal eigenvalues λ_j of the Bloch-wave operators $\mathcal{L}_\nu$ in the parameter $\nu = \mathrm{i}\gamma$. Supplementing the equation appearing in Lemma 3.3(ii) by an appropriate normalization condition, we obtain the complex boundary-value problem

$$\begin{aligned} \left[D(\partial_x + \mathrm{i}\gamma)^2 + c(\partial_x + \mathrm{i}\gamma) + a(x) - \lambda\right] u(x) &= 0 \\ \int_0^L \langle u_{\mathrm{old}}(x), u(x)\rangle \,\mathrm{d}x &= 1, \end{aligned} \tag{3.7}$$

where u_{old} is the solution at a previous continuation step or the initially supplied solution at the beginning of the computation. Note that the integral condition is evaluated in the complex field $\mathbb{C}$ and therefore selects again an element in the real two-dimensional group orbit.

If the linearization $\mathcal{L}$ arises from a translation invariant reaction-diffusion system as laid out in the introduction, then we typically need to solve the equation for the wave train and its temporal eigenvalues in tandem. Using the notation from §2 and normalizing the spatial period L to unity, we therefore consider the boundary-value problem

$$\begin{aligned} U_x &= LF(U, c), \qquad U \in \mathbb{R}^N \times \mathbb{R}^N \\ V_x &= L[F_U(U(x), c) + \lambda B - \nu]V, \qquad V \in \mathbb{C}^N \times \mathbb{C}^N \\ U(1) &= U(0) \\ V(1) &= V(0) \\ \int_0^1 \langle U'(x), U_{\mathrm{old}}(x) - U(x)\rangle \,\mathrm{d}x &= 0 \end{aligned} \tag{3.8}$$

$$\int_0^1 \langle V_{\mathrm{old}}(x), V(x)\rangle \,\mathrm{d}x \quad = \quad 1$$

corresponding to the travelling-wave ODE (2.6) and the eigenvalue problem (3.7). Here, $(U_{\mathrm{old}}, V_{\mathrm{old}})(x)$ denote the solution at a previous continuation step or the initial solution at the beginning of the continuation, and we have added appropriate phase and normalization conditions to fix an element in the group orbit of solutions. Note that the complex normalization condition for V is slightly different from the one used in (3.7) as it normalizes (u, u_x) instead of only u. While theoretically equivalent, it turns out that one or the other may be more stable in numerical computations. We also remark that computations often run more reliably when the last equation in (3.8) is replaced by the nonlinear condition

$$\int_0^1 |V(x)|^2 \,\mathrm{d}x = 1, \qquad \int_0^1 \mathrm{Im}\langle V_{\mathrm{old}}(x), V(x)\rangle \,\mathrm{d}x = 0.$$

We focus on the case where $\nu = \mathrm{i}\gamma$ is purely imaginary as this gives the essential spectrum. We remark, however, that the considerations below remain true for $\nu \in \mathbb{C}$.

If we are given a solution $(U_*, V, \lambda, \mathrm{i}\gamma)$ of (3.8), then we can continue this solution numerically as a function of $\nu = \mathrm{i}\gamma$ by using a boundary-value solver such as AUTO. The generic singularities that we may encounter during continuation of (3.8) are identical to those for constant coefficients since both problems reduce to a single analytic equation in two complex variables; in particular, we do not expect that singularities arise during continuation in γ.

It remains to find initial solutions $(V, \lambda, \mathrm{i}\gamma)$ of the eigenvalue-problem part of (3.8). Firstly note that, in the context of (3.8), $\lambda = 0$ will always be an eigenvalue of $\mathcal{L}_0$ with eigenfunction $\partial_x u_*(x)$ due to translation invariance. Thus, $(U, V, \lambda, \nu) = (U_*, \partial_x U_*, 0, 0)$ satisfies (3.8), and we can compute a curve $\lambda_0(\nu)$ of solutions to $d(\lambda, \nu) = 0$ by continuation in $\nu = \mathrm{i}\gamma$ provided $\lambda = 0$ is a simple eigenvalue of $\mathcal{L}_0$.

More generally, we may discretize the operator $\mathcal{L}_0$ with periodic boundary conditions using finite differences in space and solve the resulting matrix eigenvalue problem using packages such as LAPACK or MATLAB. Each of the resulting temporal eigenvalues λ together with its eigenfunction V can then be used, together with $\gamma = 0$, as an initial guess for (3.8).

3.4.2 Testing stability

The following lemma gives conditions that guarantee spectral stability of spatially periodic equilibria.

Lemma 3.8 *The essential spectrum of $\mathcal{L}$, with the exception of the eigenvalue $\lambda = 0$, is contained in the open left-half plane provided the following conditions hold:*

(i) The spectrum of $\mathcal{L}_0$ is contained in the open left-half plane except for the algebraically simple eigenvalue $\lambda = 0$, and the curve $\lambda_0(\mathrm{i}\gamma)$ satisfies $\lambda_0''(0) > 0$.

(ii) The origin $\lambda = 0$ is not an eigenvalue of $\mathcal{L}_\nu$ for $\nu = \mathrm{i}\gamma \notin 2\pi\mathrm{i}/L\mathbb{Z}$.

(iii) The spectrum of $\mathcal{L}$ does not intersect $\mathrm{i}\mathbb{R} \setminus \{0\}$.

To verify (i), we compute the spectrum of $\mathcal{L}_0$ and check that the eigenvalue $\lambda = 0$ is simple and that there are no other eigenvalues in the closed right-half plane. Afterward, we continue $\lambda = 0$ in $\nu = \mathrm{i}\gamma$ near $\gamma = 0$ as outlined in the preceding section to see whether $\mathrm{Re}\,\lambda_0(\mathrm{i}\gamma) < 0$ for all $\gamma \neq 0$.

Condition (ii) is equivalent to the statement that the $2N$ spatial Floquet exponents ν_j of the linear time-L map $\Phi_{\lambda=0}$ that we defined in (2.5) are non-zero except for a single simple exponent $\nu_1 = 0$ that corresponds

to the temporal eigenvalue $\lambda = 0$. The exponents ν for $\lambda = 0$ coincide with the Floquet exponents of the linearization

$$U_x = LF_U(U_*(x), c)U$$

of the travelling-wave ODE about the wave train U_*. AUTO, for instance, has subroutines that compute these Floquet exponents together with the wave train U_*.

Condition (iii) can be checked as follows: Take the spatial Floquet exponents ν_j with $j = 1, \dots, 2N$ of the wave train that were computed in the previous step at $\lambda = 0$. For each of the ν_j, we compute the corresponding Floquet eigenfunction V by solving the linear boundary-value problem

$$V_x = L[F_U(U_*(x), c) - \nu]V + \epsilon H_1(x), \qquad V(1) = V(0), \qquad \int_0^1 \langle H_2(x), V(x)\rangle \,\mathrm{d}x = 1 \tag{3.9}$$

for (V, ϵ) with $\epsilon \in \mathbb{C}$, where H_1 and H_2 are arbitrarily prescribed 1-periodic continuous functions. Note that (3.9) is linear in (V, ϵ), and it can been shown that it is uniquely solvable for any choice (H_1, H_2) except when these lie in a certain hyperspace. Once we computed a Floquet eigenfunction V_j for each ν_j at $\lambda = 0$, we continue them in ω for $\omega \in (0, |c|R_0]$ with R_0 as in §3.2 as solutions $(U_*, V_j, \mathrm{i}\omega, \nu_j)$ of (3.8). Condition (iii) is met provided $\operatorname{Re}\nu_j \neq 0$ for all $\omega \in (0, |c|R_0]$ and all j.

3.4.3 Group velocities, and Eckhaus instabilities

Quantities relevant for the interaction and stability of spatio-temporally periodic travelling waves are the group velocity

$$c_\mathrm{g} := -\frac{\mathrm{d}\lambda_0}{\mathrm{d}\nu}\Big|_{\nu=0} \in \mathbb{R},$$

which measures transport along the wave, and the coefficient

$$\frac{\mathrm{d}^2\lambda_0}{\mathrm{d}\nu^2}\Big|_{\nu=0} \in \mathbb{R}$$

which determines whether the curve $\lambda_0(\mathrm{i}\gamma)$ extends into the left or the right half-plane near the origin. Continuation of these quantities in system parameters allows us to detect sign changes of the group velocity and certain Eckhaus instabilities.

To calculate the group velocity and the above coefficient, we consider the first-order system (2.3)

$$U_x = [A(x) + \lambda B]U, \qquad U(L) = \mathrm{e}^{\mathrm{i}\gamma L}U(0) \tag{3.10}$$

with $U = (u, v) \in \mathbb{C}^{2N}$ or, equivalently, the system

$$V_x = [A(x) + \lambda B - \mathrm{i}\gamma]V, \qquad V(L) = V(0) \tag{3.11}$$

where $U = \mathrm{e}^{\mathrm{i}\gamma x}V$. We set

$$\lambda_| := \frac{\mathrm{d}\lambda_0}{\mathrm{d}\nu}\Big|_{\nu=0}, \qquad \lambda_{||} := \frac{\mathrm{d}^2\lambda_0}{\mathrm{d}\nu^2}\Big|_{\nu=0}.$$

Differentiating (3.11) with respect to $\nu = \mathrm{i}\gamma$ and evaluating the resulting equations at $\gamma = 0$, we obtain the system

$$\begin{aligned} V_|' &= A(x)V_| + [\lambda_| B - 1]V \\ V_{||}' &= A(x)V_{||} + 2[\lambda_| B - 1]V_| + \lambda_{||} BV \end{aligned} \tag{3.12}$$

on $(0, L)$ with periodic boundary conditions

$$V_|(0) = V_|(1), \qquad V_{||}(0) = V_{||}(1) \tag{3.13}$$

for $V_| := \partial_\nu V$ and $V_{||} := \partial_\nu^2 V$ both in $\mathbb{R}^{2N}$ and $(\lambda_|, \lambda_{||}) \in \mathbb{R}^2$. Lastly, we add the boundary conditions

$$\int_0^1 \langle V(x), V_|(x)\rangle \, \mathrm{d}x = 0, \qquad \int_0^1 \langle V(x), V_{||}(x)\rangle \, \mathrm{d}x = 0, \tag{3.14}$$

which ensure that both $V_|$ and $V_{||}$ are L^2-orthogonal to the null space of the ODE for V. We mention that the scalar products in the integral conditions can be replaced by the PDE scalar products which sometimes appear to be computationally more stable and reliable.

The system (3.8)-(3.14) with $\lambda = \nu = 0$ can now be solved uniquely for (U, c), $(V, V_|, V_{||})$ and $(\lambda_|, \lambda_{||})$.

In fact, using nontrivial solutions $V(x)$ and $W(x)$ of

$$V_x = A(x)V, \qquad V(0) = V(1), \qquad W_x = -A(x)^t W, \qquad W(0) = W(1)$$

and finding $\tilde{V}(x)$ so that

$$\tilde{V}_x = A(x)\tilde{V} + (\lambda_| B - 1)V, \qquad \tilde{V}(0) = \tilde{V}(1),$$

we have

$$\lambda_| = \frac{\langle W, V\rangle_{L^2}}{\langle W, BV\rangle_{L^2}}, \qquad \lambda_{||} = \frac{\langle W, 2(\lambda_| B - 1)\tilde{V}\rangle_{L^2}}{\langle W, BV\rangle_{L^2}}.$$

3.5 Implementation in AUTO

We now discuss briefly how the strategies that we outlined above can be implemented in the continuation package AUTO and refer to names of routines and constants as given in [2]. Since AUTO uses only real arithmetic, dimension counting will always be done over *real numbers* (unless explicitly stated otherwise).

3.5.1 Periodic coefficients

Implementing the system (3.8) in AUTO works as follows.

The constants file: Equation (3.8) is a boundary-value problem, and we therefore set `ips=4`. The ODEs appearing in (3.8) involve $6N$ real unknowns, namely $(U, V) \in \mathbb{R}^{2N} \times \mathbb{C}^{2N}$, and we thus set `ndim=6N`. We have `nbc=6N` real boundary conditions and `nint=3` real integral conditions. Since the ODEs can be solved uniquely upon choosing initial conditions, we have effectively $6N + 3$ real equations and need therefore the same number of variables plus one for continuation which gives $6N + 4$. In addition to the $6N$ initial data for (U, V), we have five real parameters at our disposal, namely $c, L, \gamma \in \mathbb{R}$ and $\lambda \in \mathbb{C}$. Thus, we may fix the period L and use the four parameters $\gamma, c \in \mathbb{R}$ and $\lambda \in \mathbb{C}$ for continuation by setting `nicp=4` and specifying the four parameters in the array `icp`. It may be helpful for convergence to increase the number of Newton iterations `itnw` from its default value.

The equations file: The unknowns $(U, \mathrm{Re}\, V, \mathrm{Im}\, V) \in \mathbb{R}^{2N} \times \mathbb{R}^{2N} \times \mathbb{R}^{2N}$ are set to the variables `U(1)`,...,`U(6N)`. The period L is stored in `par(11)`, and we use `par(1)`,...,`par(4)` for $c, \gamma, \mathrm{Re}\,\lambda, \mathrm{Im}\,\lambda$. The periodic boundary conditions are defined in the subroutine `bcnd` via

```
do j=1,ndim
   fb(j) = U0(j) - U1(j)
end do
```

The integral conditions are defined in `icnd`. We set

```
fi(1) = 0.0
do j=1,ndim/3
   fi(1) = fi(1) + UPOLD(j) * (UOLD(j)-U(j))
end do
```

for the phase condition of the wave train U, and use

```
fi(2) = -1.0
fi(3) = 0.0
do j=ndim/3+1,2*ndim/3
   fi(2) = fi(2) + U(j)*U(j) + U(j+ndim/3)*U(j+ndim/3)
   fi(3) = fi(3) + UOLD(j)*U(j+ndim/3) - UOLD(j+ndim/3)*U(j)
end do.
```

for the normalization of the eigenfunction V.

Initial data: We assume that the period L, the wave train $U_* = (u_*, u_*')$ and the associated wave speed c are known. These can be obtained, for instance, from direct PDE simulations or from continuation in the travelling-wave ODE (2.6) beginning at a Hopf bifurcation point. We also assume that we found initial solutions for λ, γ and the associated eigenfunction V (see §3.4.1). This information needs to be stored in the subroutine `stpnt` or an external data file that can be read by AUTO (see [2]). It is recommended to scale the initial guess for the eigenfunction to have norm one so that it satisfies the integral condition; otherwise, convergence may be be quite slow.

Solving (3.9) and (3.12): We discuss now how equation (3.9) is solved to get the Floquet eigenfunction V for a given Floquet exponent ν. First, we pick functions H_1 and H_2 (for instance, constant functions). Note that (3.9) involves two real integral conditions and a real two-dimensional parameter ϵ. We fix ν and continue instead in the real two-dimensional ϵ and the unused dummy parameter `par(9)`: continuation in a dummy parameter in AUTO allows us to solve a linear or nonlinear system through Newton's method. Next, we continue to $\operatorname{Re}\epsilon = 0$ using $\operatorname{Im}\nu$ as additional free parameter. Lastly, we continue to $\operatorname{Im}\epsilon = 0$ using ν as free parameter.

Equation (3.12) is solved analogously. It is affine in the unknowns $(V_|, V_{||}, \lambda_|, \lambda_{||}) \in \mathbb{R}^{2N} \times \mathbb{R}^{2N} \times \mathbb{R}^2$ and almost any initial guess (for instance, a constant function) for $(V_|, V_{||}, \lambda_|, \lambda_{||})$ will give the correct solution by continuing in the dummy parameter `par(9)` and the active parameters $(\lambda, \lambda_|, \lambda_{||}) \in \mathbb{C} \times \mathbb{R}^2$, starting at $\lambda = \nu = 0$. We recommend to exclude $V_|, V_{||}$ from the pseudo-arclength computation by setting `nthu=8` succeeded by $4N$ lines of the form `<index of component> 0`.

3.5.2 Constant coefficients

The implementation for constant coefficients is similar to the one for periodic coefficients discussed above. While the eigenvalue problem (3.3) is only an algebraic equation, it is recommended to implement it as a boundary-value problem as in §3.5: this is done by setting `ips=4` and choosing `ntst=1` and `ncol=2`. In the following, we shall only comment on the differences to the implementation for periodic coefficients.

The constants file: Unless the equilibrium is to be continued in a parameter, we do not need to solve the nonlinear problem simultaneously. In this case, we then have two integral conditions, three free parameters

($\gamma \in \mathbb{R}$ and $\lambda \in \mathbb{C}$), and the vector $u \in \mathbb{C}^N$ stored in `U(1)`,...,`U(2N)` in AUTO. (It may also be convenient to use the files from the periodic case in the first order formulation with $U \in \mathbb{C}^{2N}$.) We recommend to disable mesh adaption by setting `iad=0`.

Initial data: Initial data for λ, ν and the eigenvector u (or $U = (u, \frac{du}{dx})$) can be imported from root-solving routines in packages such as MAPLE or MATHEMATICA applied to the dispersion relation $d(\lambda, \nu) = 0$ for a fixed value of either λ or ν.

4 Absolute spectra

4.1 Definition and characterization of the absolute spectrum

As outlined in the introduction, the absolute spectrum arises naturally as follows: Take the linearization $\mathcal{L}$ about an asymptotically homogeneous or periodic travelling wave and compute its spectrum on the interval $(-\ell, \ell)$ with fixed separated boundary condition at $x = \pm\ell$. The resulting spectra will depend on ℓ and on the boundary conditions. It is proved in [9] that these spectra converge, uniformly on compact subsets of $\mathbb{C}$ and in the symmetric Hausdorff distance, to a limiting spectral set as $\ell \to \infty$. The continuous (non-discrete) part of the limiting set is given by the absolute spectrum Σ_{abs}, defined below in Definition 1, which does *not* depend on the boundary conditions: As $\ell \to \infty$, each element of the absolute spectrum is approached by infinitely many eigenvalues of $\mathcal{L}$ which therefore cluster near the absolute spectrum. We emphasize that the results in [9], even though mostly formulated for constant coefficients, are valid for periodic coefficients.

Definition 1 *For constant coefficients, we define the generalized absolute spectrum Σ^m_{abs} with Morse index m as the set of those $\lambda \in \mathbb{C}$ for which*

$$\operatorname{Re}\nu_1 \geq \ldots \geq \operatorname{Re}\nu_m = \operatorname{Re}\nu_{m+1} \geq \ldots \geq \operatorname{Re}\nu_{2N}$$

where ν_j are the $2N$ roots of $d(\lambda, \nu)$ repeated with multiplicity. The generalized absolute spectrum

$$\Sigma^*_{\text{abs}} := \bigcup_{m=1}^{2N-1} \Sigma^m_{\text{abs}}.$$

is the union over all indices m, and the absolute spectrum is defined as

$$\Sigma_{\text{abs}} := \Sigma^N_{\text{abs}}.$$

For periodic coefficients, we use the same definition with the eigenvalues ν replaced by the Floquet exponents of Φ_λ.

The notation Σ_{abs} and Σ^N_{abs} will be used interchangeably for the *absolute spectrum*. The generalized absolute spectrum with Morse index different from N is usually meaningless for spectral properties of $\mathcal{L}$ from (2.1). It is, however, a natural first step towards the computation of the absolute spectrum. Note that each Σ^m_{abs} is typically the union of curve segments that are glued together at singularities that we shall discuss in detail below. First, we note the absolute spectrum is also bounded to the right:

Remark 4.1 *For both (C) and (P), a straightforward scaling result shows that for each fixed $\delta \in (0, \frac{\pi}{2})$ there is a constant $R > 0$ so that Σ^N_{abs} does not contain any elements λ with $|\lambda| > R$ and $|\arg\lambda| < \frac{\pi}{2} + \delta$.*

The characterization of Σ^*_{abs} in Definition 1 allows us to reformulate Σ^*_{abs} using the system

$$d(\lambda,\nu_1)=0, \qquad d(\lambda,\nu_2)=0, \qquad \nu_2-\nu_1=\mathrm{i}\gamma \tag{4.1}$$

with $\gamma\in\mathbb{R}$. We see that $\lambda\in\Sigma^*_{\text{abs}}$ if either (λ,ν_1,ν_2) are solutions of (4.1) for some nonzero real γ or else if λ and $\nu_1=\nu_2$ are solutions of (4.1 with $\partial_\nu d(\lambda,\nu_1)=0$. Setting $\nu=\nu_1$ and $\nu_2=\nu+\mathrm{i}\gamma$, we can remove the singularity of (4.1) at $\gamma=0$ by considering the system

$$\mathcal{A}(\lambda,\nu;\gamma)=\left(d(\lambda,\nu),\frac{d(\lambda,\nu)-d(\lambda,\nu+\mathrm{i}\gamma)}{\mathrm{i}\gamma}\right)=0 \tag{4.2}$$

so that $\mathcal{A}:\mathbb{C}\times\mathbb{C}\times\mathbb{R}\to\mathbb{C}^2$. Thus, $\lambda\in\Sigma^*_{\text{abs}}$ if, and only if, $(\lambda,\nu;\gamma)$ satisfies (4.2). We shall call solutions (λ,ν) of $\mathcal{A}(\lambda,\nu;0)=0$ *double roots*.

4.2 Constant coefficients

Computationally, it is more reliable and convenient to replace the dispersion relations $d(\lambda,\nu)$ by the original algebraic equations. Using the definition

$$\mathcal{D}(\lambda,\nu):=D\nu^2+c\nu+a_0-\lambda,$$

the system $\mathcal{A}(\lambda,\nu;\gamma)=0$ is equivalent to solving

$$\mathcal{D}(\lambda,\nu)u=0, \qquad [D(2\nu+\mathrm{i}\gamma)+c](u+\mathrm{i}\gamma v)+\mathcal{D}(\lambda,\nu)v=0, \tag{4.3}$$

together with the normalization

$$\langle u_{\text{old}},u\rangle=0, \qquad \langle v_{\text{old}},u\rangle-\langle u_{\text{old}},v\rangle-\mathrm{i}\gamma\langle v_{\text{old}},v\rangle=0. \tag{4.4}$$

4.2.1 Continuation within the generalized absolute spectrum

We now collect several properties of the system $\mathcal{A}(\lambda,\nu;\gamma)=0$ before we return to solving (4.3)-(4.4).

For each isolated solution (λ,ν) of $\mathcal{A}(\lambda,\nu;\gamma)=0$ for some fixed $\gamma\geq 0$, we can define its multiplicity to be the (real) Brouwer degree $\deg(\mathcal{A}(\cdot,\cdot;\gamma),0)$ in the variable (λ,ν), evaluated at the solution (λ,ν).

Lemma 4.2 *The multiplicity is nonnegative. Furthermore, the degree of $(\lambda,\nu)=0$ at $\gamma=0$ is one precisely when $\partial_\lambda d(0,0)\neq 0$ and $\partial_{\nu\nu}d(0,0)\neq 0$.*

Proof. Since the derivative $\partial_{(\lambda,\nu)}\mathcal{A}$ is complex linear, it has a nonnegative determinant when considered as a real 4×4 matrix which proves the first claim. The second statement follows since $\partial_{(\lambda,\nu)}\mathcal{A}(0)$ is, in this case, block-diagonal with diagonal entries given as non-zero complex multiples of the identity, such that $\det\partial_{(\lambda,\nu)}\mathcal{A}(0)>0$. ∎

We call solutions for $\gamma=0$ with multiplicity one *simple double roots*. If a solution is not isolated, we say it has multiplicity ∞.

In the following, we consider various homotopies by allowing the coefficients D, c, a_0 and γ to depend on a homotopy parameter $\tau\in[0,1]$. The resulting functions will be denoted by $\mathcal{A}_\tau(\lambda,\nu)$, omitting the dependence on $\gamma=\gamma(\tau)$. The homotopy invariance of the Brouwer degree gives the following result.

Lemma 4.3 *The number (λ,ν) of roots of $\mathcal{A}_\tau(\lambda,\nu)$ inside a ball $G\subset\mathbb{C}^2$ is independent of τ provided there are no roots on the boundary ∂G for each $\tau\in[0,1]$. Here, solutions are counted with multiplicity.*

Next, we prove that the assumption in the preceding lemma is automatically met provided the ball G has sufficiently large diameter.

Lemma 4.4 *If the diffusion coefficients are pairwise distinct so that $d_i \neq d_j$ for $i \neq j$, then there exists a number $R > 0$, depending only on $|D|$, $|a_0|$, $|c|$ and $|\gamma|$, such that every solution (λ, ν_1, ν_2) of (4.1) satisfies*

$$|\lambda| + |\nu_1| + |\nu_2| \leq R.$$

Proof. A straightforward estimate of the linear equation $\mathcal{D}(\lambda, \nu)u = 0$ shows that $|\nu| \equiv \pm\sqrt{\lambda/d_i}$ for some i as either λ or ν tend to infinity. Since $d_i \neq d_j$ for $i \neq j$, this implies $|\operatorname{Im}(\nu_1 - \nu_2)| \to \infty$ whenever $\operatorname{Re}\nu_1 = \operatorname{Re}\nu_2$, and therefore $|\gamma| \to \infty$. ∎

Lemma 4.5 *Assume that $d_i \neq d_j$ for $i \neq j$, then there are precisely $\binom{2N}{2}$ double roots, i.e. solutions to $\mathcal{A}(\lambda, \nu; 0) = 0$, when counted with multiplicity.*

Proof. We choose a homotopy of $\mathcal{A}(\lambda, \nu; 0) = 0$ to the equation with $c = 0$ and $a = \operatorname{diag}(a_j)$. On account of Lemmata 4.3 and 4.4, the number of roots of $\mathcal{A}_\tau(\lambda, \nu; 0)$ does not change during the homotopy. For the resulting diagonal equation, there are N roots $(\lambda, \nu) = (d_j, 0)$ which are easily seen to have multiplicity one. The remaining roots are solutions to

$$d_i\nu^2 + a_i - \lambda = 0, \qquad d_j\nu^2 + a_j - \lambda = 0,$$

that is, to

$$\lambda = d_i\nu^2 + a_i, \qquad \nu^2 = -\frac{a_i - a_j}{d_i - d_j}$$

for a given pair (i, j) with $1 \leq i < j \leq N$. Choosing the a_j appropriately, the above system has $N(N-1)$ distinct solutions. We claim that each solution has Brouwer degree equal to 2. Indeed, differentiate the dispersion relation

$$d(\lambda, \nu) = \Pi_{j=1}^N[\lambda - d_j\nu^2 - a_j]$$

and compute the Taylor jet at the solutions (λ_*, ν_*):

$$d(\lambda, \nu) = a(\lambda - \lambda_*)^2 - b(\nu - \nu_*)^2 + \mathrm{O}(3)$$

with $a \neq 0$. In particular, $d(\lambda, \nu) + \varepsilon$ has two simple double roots at $\lambda = \lambda_* \pm \sqrt{\varepsilon/a} + \mathrm{O}(\epsilon)$ and $\nu = \nu_*$. The additivity and homotopy invariance of the degree shows that the multiplicity is two. Altogether, we have found $N + 2N(N-1) = 2N(2N-1)/2$ roots which proves the lemma. ∎

As an immediate consequence, we conclude that the generalized absolute spectrum consists of at most $\binom{2N}{2}$ curves that are parameterized by γ.

Corollary 4.6 *The generalized absolute spectrum is given by*

$$\Sigma^*_{\mathrm{abs}} = \bigcup_{\gamma \geq 0} \left\{ \lambda_j(\gamma);\ j = 1, \ldots, \binom{2N}{2} \right\},$$

where $\lambda_j(\gamma)$ denotes the λ-component of the solutions to $\mathcal{A}(\lambda, \nu; \gamma) = 0$. Moreover, $\lambda_j(\gamma)$ can be chosen to be continuous in γ. In particular, Σ^*_{abs} consists of at most $\binom{2N}{2}$ connected components, each containing a double root and the point at infinity (when considered on $\overline{\mathbb{C}}$).

Proof. The representation of Σ^*_{abs} follows from the previous discussion and the homotopy invariance of the degree in a ball of radius R for each fixed finite γ, and therefore for all γ. To show continuity, we have to pick continuous curves $\lambda_j(\gamma)$ out of the setwise continuous continuum of solutions to $\mathcal{A}(\lambda,\nu)=0$. We therefore look at the family of perturbed problems $\mathcal{A}=\varepsilon^{(1)}\lambda+\varepsilon^{(2)}\nu$. By Thom's transversality theorem, there exist sequences $\varepsilon_k=(\varepsilon_k^{(1)},\varepsilon_k^{(2)})\to 0$ such that the solution sets $\lambda_j^k(\gamma)$ form smooth curves. By continuity of the solution set, and finiteness of the index set j, we may pick a subsequence k_ℓ such that the curves $\lambda_j^{k_\ell}$ converge uniformly in γ to the solution curves of the limiting problem, thus providing us with a continuous labelling of the solutions $\lambda_j(\gamma)$ for the original problem. ∎

To summarize, to compute the generalized absolute spectrum, it suffices to calculate all double roots and to subsequently continue the curves of Σ^*_{abs} that emanate from the double roots in γ from $\gamma=0$ to $\gamma=\infty$.

We remark that double roots may coalesce in certain situations:

Lemma 4.7 *If a is triangular and $n\geq 2$, then there are at least two degenerate double roots (λ_*,ν_*) of the dispersion relation which are double roots with respect to both ν and λ so that*

$$d(\lambda_*+\lambda,\nu_*+\nu)=\alpha_2\lambda^2+\beta_2\nu^2+\mathrm{O}(|\lambda|^3+|\nu|^3).$$

Proof. It suffices to consider $n=2$, $D=(1,\delta)$ with $\delta\neq 0$, and $a=\left(\begin{smallmatrix}a_1 & *\\ 0 & a_2\end{smallmatrix}\right)$ in which case the dispersion relation is equal to $d(\lambda,\nu)=d_1(\lambda,\nu)d_2(\lambda,\nu)=0$ with $d_1(\lambda,\nu)=\nu^2+c\nu-\lambda+a_1$ and $d_2(\lambda,\nu)=\delta\nu^2+c\nu-\lambda+a_2$. In particular, there are $\binom{4}{2}=6$ double roots for $\delta\neq 1$ which satisfy $d=0$ and $\partial_\nu d=(\partial_\nu d_1)d_2+d_1\partial_\nu d_2=0$.

The solutions to $d_1=0$ and $d_2=0$ are given by $\lambda_1=\nu^2+c\nu+a_1$ and $\lambda_2=\delta\nu^2+c\nu+a_2$, respectively, where ν is arbitrary. These give rise to spatial double roots provided $d_2(\lambda_1,\nu)=0$ or $d_1(\lambda_2,\nu)=0$, respectively, that is, when $\delta\nu^2+c\nu-(\nu^2+c\nu+a_1)+a_2=0$ or $\nu^2+c\nu-(\delta\nu^2+c\nu+a_2)+a_1=0$. This is the case for $\nu_j^{\pm}=\pm\sqrt{(-1)^j\frac{a_2-a_1}{1-\delta}}$. The remaining two of the six double roots are the roots $\nu_1=-\frac{c}{2}$ and $\nu_2=-\frac{c}{2\delta}$ of the dispersion relations d_1 and d_2, respectively. ∎

If some of the diffusion coefficients are equal ($d_i=d_j$ for appropriate indices $i\neq j$), we cannot a priori exclude that branch points 'disappear' at infinity. In fact, in the explicit decoupled model problem that we utilized in the proof of Lemma 4.5, a double branch point 'crosses' the point at infinity when d_i-d_j crosses zero.

4.2.2 Testing absolute stability

We shall show that, for constant-coefficient operators, the absolute spectrum Σ^N_{abs} is connected in $\bar{\mathbb{C}}$. Since Remark 4.1 shows furthermore that it lies in an acute sector that opens up along the negative real axis, it suffices to check whether the absolute spectrum has a nonzero intersection with the imaginary axis to establish stability or instability.

Lemma 4.8 *The absolute spectrum Σ^N_{abs} is connected in $\bar{\mathbb{C}}$ and contains the point at infinity. Furthermore, the absolute spectrum Σ^N_{abs} is contained in the open left half-plane if, and only if, it does not intersect the imaginary axis.*

Proof. We argue by contradiction. Thus, suppose that $\tilde{\Sigma}$ is a non-empty, compact subset of Σ^N_{abs} so that there is a smooth Jordan curve Γ in $\mathbb{C}$ with $\Gamma\cap\Sigma^N_{\text{abs}}=\emptyset$ and $\operatorname{int}\Gamma\cap\Sigma^N_{\text{abs}}=\tilde{\Sigma}$. The idea is to show that the spectrum of $\mathcal{L}$ on $(-\ell,\ell)$ with appropriate boundary conditions cannot accumulate on $\tilde{\Sigma}$ in contradiction to

[9, Theorem 5]. Since Γ does not intersect the absolute spectrum with Morse index N, the eigenvalues ν_j of $A+\lambda B$ satisfy

$$\operatorname{Re}\nu_1 \le \ldots \le \operatorname{Re}\nu_N < \operatorname{Re}\nu_{N+1} \le \ldots \le \operatorname{Re}\nu_{2N}$$

for all $\lambda \in \Gamma$. We denote the N-dimensional generalized eigenspaces associated with the N leftmost and rightmost eigenvalues by $E^{\mathrm{s}}(\lambda)$ and $E^{\mathrm{u}}(\lambda)$, respectively: These spaces are well defined, unique and analytic in λ for λ in a neighbourhood $\mathcal{U}$ of Γ. Next, pick $\lambda_0 \in \Gamma$ and an N-dimensional subspace E^{bc} with

$$E^{\mathrm{bc}} \oplus E^{\mathrm{u}}(\lambda) = \mathbb{C}^N, \qquad E^{\mathrm{bc}} \oplus E^{\mathrm{s}}(\lambda) = \mathbb{C}^N \tag{4.5}$$

for $\lambda = \lambda_0$. Analyticity then implies that (4.5) is true for all $\lambda \in \mathcal{U}$ except possibly for finitely many λ. Redefining Γ if necessary, we can therefore assume that (4.5) is true for all $\lambda \in \Gamma$.

We set our boundary conditions by choosing a matrix $Q_-^{\mathrm{bc}} = Q_+^{\mathrm{bc}}$ with null space equal to E^{bc}. Equation (4.5) shows that [9, Hypothesis 7] is met, and [9, Proposition 5] now asserts that there are numbers $M \ge 0$ and $\ell_* \gg 1$ such that the spectrum of $\mathcal{L}$ on $(-\ell,\ell)$ with the boundary conditions (1.3) contains precisely M elements in the interior of Γ and does not intersect Γ for $\ell \ge \ell_*$. We emphasize that (4.5), and therefore the above statement, remains true if we change E^{bc}, A, and B slightly.

Next, pick an element λ_1 in the non-empty set $\tilde{\Sigma}$. Upon transforming the matrix $A+\lambda_1 B$ into Jordan normal form, it is easy to see that there are matrices C_0 and C_1 of arbitrarily small norm so that the eigenvalues ν_j of

$$A + \lambda_1 B + C_0 + (\lambda - \lambda_1)C_1 \tag{4.6}$$

satisfy

$$\operatorname{Re}\nu_1 \le \ldots \le \operatorname{Re}\nu_{N-1} < \operatorname{Re}\nu_N = \operatorname{Re}\nu_{N+1} < \operatorname{Re}\nu_{N+2} \le \ldots \le \operatorname{Re}\nu_{2N}, \qquad \operatorname{Im}\nu_N \neq \operatorname{Im}\nu_{N+1} \tag{4.7}$$

at $\lambda = \lambda_1$ and

$$\frac{\mathrm{d}\operatorname{Im}(\nu_N - \nu_{N+1})}{\mathrm{d}\lambda}\Big|_{\lambda=\lambda_1} \neq 0. \tag{4.8}$$

In particular, we may choose C_0 and C_1 so small that the statements in the previous paragraph are also true for (4.6). On the other hand, (4.7) and (4.8) show that [9, Hypothesis 8] is satisfied near $\lambda = \lambda_1$, and [9, Theorem 5] now implies that the number of eigenvalues of $\mathcal{L}$ (on $(-\ell,\ell)$ with the boundary conditions (1.3)) in a small disk centered at λ_1 becomes unbounded as $\ell \to \infty$. This contradicts the statement established before that this number is equal to M which is independent of ℓ. The second statement of the lemma follows from Remark 4.1. ∎

4.2.3 Generic singularities

The generalized absolute spectrum Σ^*_{abs} typically does not admit any singularities. Upon shifting, curves of generalized absolute spectrum pass through zero where they emanate from double roots $\lambda \equiv \alpha\nu^2$ with $\nu_1 = -\nu_2 = \pm\mathrm{i}\gamma/2$ along $\lambda = -\gamma^2\alpha/4$. However, even though we may continue curves in Σ^*_{abs} smoothly, the Morse index m may jump along these curves. This occurs typically at *triple points*, where $\operatorname{Re}\nu_{j+1} = \operatorname{Re}\nu_{j+2} = \operatorname{Re}\nu_{j+3}$, $\operatorname{Im}\nu_{j+1} > \operatorname{Im}\nu_{j+2} > \operatorname{Im}\nu_{j+3}$. One expects these conditions to hold at discrete points on the generalized absolute spectrum. Typically, $\lambda = \lambda_{\mathrm{triple}} + b_l(\nu-\nu_l) + \mathrm{O}(|\nu-\nu_l|^2)$ for $l = j, j+1, j+2$ near these singularities, and the resulting bifurcation picture is readily computed under the assumption that the coefficients b_l are different from each other (see Figure 1).

The Morse index drops from $j+1$ to j along two of the curves as they cross the singularity. Between these two curves that enter the generalized absolute spectrum, there is a curve of generalized absolute spectrum that crosses the singularity along which the Morse index increases. The Morse index increase happens along

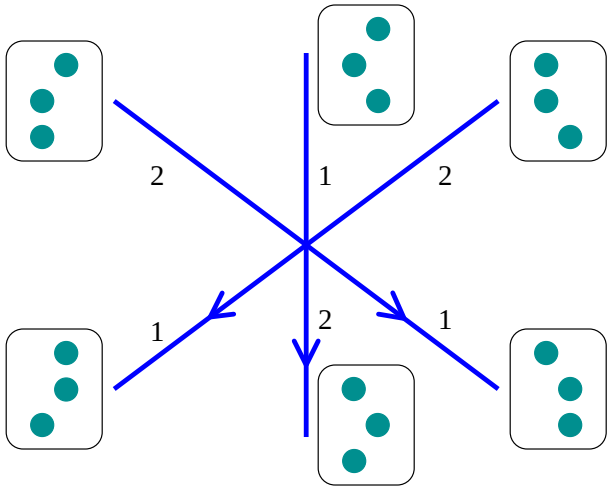

Figure 1: *A triple-point singularity of the generalized absolute spectrum in the complex λ-plane. Curves are oriented by* $\operatorname{sgn}(\gamma)$*, numbers are Morse indices minus j. Insets show relevant spatial eigenvalues.*

the curve where $\operatorname{Re}\nu_1 = \operatorname{Re}\nu_3$, i.e. where the difference of imaginary parts is given by the sum of the two other differences of imaginary parts.

Note that if we insist on following curves with constant Morse index (rather than preserving smoothness during the continuation), then we are losing a curve with Morse index $j+1$ and creating a curve with Morse index j. Moreover, if we follow curves with Morse index j, the parameter γ *jumps down* as we cross the singularity. In particular, local considerations do not enforce curves of constant Morse index to continue to $\gamma = \infty$, although we may well be able to continue them in λ. We emphasize that the absolute spectrum is nevertheless connected in $\bar{\mathbb{C}}$, see Lemma 4.8.

The singularity $\mathrm{d}\nu_1/\mathrm{d}\lambda = \mathrm{d}\nu_2/\mathrm{d}\lambda$ at ν_j^*, $j = 1, 2$, in the generalized absolute spectrum typically requires an additional parameter, but can be observed on the real axis without external parameter. To leading order, we find $\nu_j \equiv \nu_j^* + a\lambda + b_j\lambda^2$, $j = 1, 2$, from the dispersion relation and therefore

$$\operatorname{Re}(\nu_1 - \nu_2) = \operatorname{Re}[(b_1 - b_2)\lambda^2] = 0$$

with solutions forming a rectangular cross to leading order, where γ increases towards the singularity on one of the curves and it decreases towards the singularity on the other perpendicular curve. The Morse indices are the same on all four curves. This occurs, for instance, on a real interval of Σ^*_{abs} that is bounded by two double roots at the endpoints.

Due to the symmetry of spatial eigenvalues with respect to the real axis there is also the possibility of two pairs of complex conjugate spatial eigenvalues, in which case we expect 12 curves of Σ^*_{abs} meet in one point, four of which are real intervals.

4.3 Periodic coefficients

The initial setup for periodic coefficients is similar. The dispersion relation is now given by

$$d(\lambda, \nu) = \det[\Phi_\lambda - \mathrm{e}^{\nu L}],$$

and we shall use the regularized system

$$\mathcal{D}(\lambda, \nu)u = 0, \qquad [D(2(\partial_x + \nu) + \mathrm{i}\gamma) + c](u + \mathrm{i}\gamma v) + \mathcal{D}(\lambda, \nu)v = 0, \tag{4.9}$$

where

$$\mathcal{D}(\lambda,\nu) = D(\partial_x+\nu)^2 + c(\partial_x+\nu) + a(x) - \lambda, \tag{4.10}$$

together with the normalization conditions

$$\begin{aligned} \int_0^L \langle u_{\text{old}}, u\rangle \,\mathrm{d}x &= 1 \\ \int_0^L \left[\langle v_{\text{old}}, u\rangle - \langle u_{\text{old}}, v\rangle - \mathrm{i}\gamma\langle v_{\text{old}}, v\rangle\right]\mathrm{d}x &= 0 \end{aligned} \tag{4.11}$$

for u and v. It suffices here to consider $\gamma \in [0, \pi/L)$.

Regarding instability of the absolute spectrum, we can conclude that the existence of an unstable isola of essential spectrum implies unstable absolute spectrum provided it lies in the boundary of the component of the resolvent set where the Morse index of the period map Φ_λ is N. This observation is a consequence of the more general fact that isolas of essential spectrum contain absolute spectrum with a certain Morse index (see [6, Theorem 3.3] and [7] for details).

Continuing a curve of (generalized) absolute spectrum from double roots proceeds as for the constant coefficients. However, there is an infinite number of double roots for $\gamma = 0$ even though each bounded region of the complex plane typically contains only finitely many. Compared to the constant-coefficient case, it is also much more problematic to find double roots in the first place: in fact, we do not know of any systematic way of locating double roots in a given region of the complex plane.

Similar to constant coefficients, there is the possibility that the absolute spectrum consists of curve segments of generalized absolute spectrum. We would therefore need to compute Σ^*_{abs} and determine the Morse index on each segment. We conjecture, however, that for periodic coefficients most of the absolute spectrum consists of isolated smooth curves.

We next describe possible strategies for locating elements of the (generalized) absolute spectrum which involve continuation of (3.8) in the real part η of $\nu = \eta + \mathrm{i}\gamma$, which corresponds to posing $\mathcal{L}$ in an exponentially weighted space with weight η.

Firstly, consider an intersection point of two curve segments of essential spectrum, possibly for $\eta \neq 0$. Unless this point is a root of $\partial_\lambda d(\lambda,\nu)$, it lies in the generalized absolute spectrum, because two Floquet exponents have the same real part, and it can be used as a starting point for continuation. In fact, a Jordan curve of essential spectrum that does not contain further essential spectrum continues in η either to a self intersecting curve or to a double root, see [7] for details.

Secondly, we discuss the special case of generalized absolute spectrum on the real axis. At $\lambda \in \mathbb{R}$, a Floquet exponent ν is either real or there is the complex conjugate exponent $\overline{\nu}$. If $\nu \in \mathbb{R}$, then $\mathrm{Im}(\nu) = mi\pi$ for $m \in \mathbb{Z}$, i.e. it is a positive or negative Floquet multiplier.

In case of a distinct pair of complex conjugate Floquet exponents, a slight change in the real part of λ or $\eta = \mathrm{Re}(\nu)$ does not change the complex conjugate relation and so there is in fact an interval of $\mathbb{R}\cap\Sigma^*_{\text{abs}}$. Note that an endpoint of this interval is a double root. Conversely, continuation of ν in λ on the real axis may lead to double roots in the generalized absolute spectrum. Note that by symmetry of Floquet exponents, the computation of real intervals only requires continuation of one Floquet exponent, i.e. (3.8) with $\nu = \eta + \mathrm{i}\gamma$.

In the other case, there are two real Floquet exponents with equal real part and imaginary parts $\gamma = 0$ and $\gamma = \pi$, respectively. Since varying λ along the real axis will leave the Floquet exponents real, changing the imaginary part of λ will only change the imaginary part of the Floquet exponents to leading order, by the Cauchy Riemann equations. The corresponding curve of absolute spectrum intersects the real axis with a vertical tangent. Conversely, for $\lambda \in \mathbb{R}$ the continuation in η of a pair of Floquet multipliers with opposite sign may lead to the location of such a crossing point.

Other typical singularities of the absolute spectrum on the real axis are as described in §4.2.3, keeping in mind that signs of Floquet multipliers may differ.

We refer to §5 and [6, Chapter 4.4] as well as [7] for examples where exponential weights have been used to locate absolute spectrum.

4.4 Continuation, and implementation in AUTO

In the case of constant coefficients, we first calculate all double roots (λ, ν), i.e. all roots of $\mathcal{A}(\lambda, \nu; 0) = 0$, and subsequently nontrivial solutions u and v of the linear equation (4.3). Starting from each of these at most $\binom{2N}{2}$ points, see corollary 4.6, we then continue solutions of (4.3)-(4.4) in γ.

Afterward, we reconstruct the Morse indices on all curve segments of Σ^*_{abs} between triple points and double roots by computing all $2N$ solutions of $\mathcal{A}(\lambda, \nu; \gamma) = 0$ at all double roots and triple points (or at arbitrary test points on each segment). Alternatively, we could compute all $2N$ solutions ν_j of $\mathcal{D}(\lambda, \nu_j)u_j = 0$ and (4.3)-(4.4) simultaneously, though this is computationally much more expensive.

We remark that it is not necessary to use the regularized system (4.3)-(4.4) away from double roots. Instead, it may be convenient for the implementation to use the equations $\mathcal{D}(\lambda, \nu)u_1 = 0$ and $\mathcal{D}(\lambda, \nu + \mathrm{i}\gamma)u_2 = 0$.

Except for the location of double roots, these remarks equally apply to periodic coefficients and (4.9)-(4.11). For consistency with this case, we describe the setup in AUTO for (4.3)-(4.4) as a first order system and boundary value problem, so there are $2N + 2N$ complex equations. This way the same equation file of AUTO can be used.

The constants file: We cast both (4.3) and (4.9) as `ndim=8N` real algebraic equations with periodic boundary conditions, `bcnd=8N`, and `icnd=4` real integral conditions to normalize. The `nicp=5` free parameters are $\lambda, \nu \in \mathbb{C}$ and $\gamma \in \mathbb{R}$. It is useful for subsequent computations to view $\gamma = \mathrm{Im}(\nu_2)$ and include $\mathrm{Re}(\nu_2)$ in the implementation.

For the case of constant coefficients, eigenfunctions are spatially constant, so we set `ntst=1` and `ncol=2`. We recommend to disable mesh adaption by setting `iad=0`, and to exclude the vector v in (4.3)-(4.4) from the pseudo-arclength computation. For this set `nthu=4` succeeded by $2N$ lines of the form `<index of component> 0`.

The equations file: We recommend to implement the operator $\mathcal{D}(\lambda, \nu)$ in a new subroutine called from the subroutine `func`, because (4.3) and (4.9) require two evaluations. Also this makes it easy to simultaneously continue all eigenvalues and thereby the Morse index, if feasible. The current Morse index can then be stored in an additional parameter to check changes. Boundary and integral conditions are implemented in the subroutine `bncd` and `icnd` as described previously in §3.5.

Initial data: For constant coefficients, we use double roots as described above and set the data in the subroutine `stpnt`. For periodic coefficients, initial points in the generalized absolute spectrum are often found by continuing single Floquet exponents in exponential weights to a point where two of these have the same real part. To improve convergence of the initialization, we recommend to join both eigenfunctions and the nonlinear solution into a single data file and rescale to the same discretization grid. The program `@fc` converts such a file to AUTO format and reads initial parameters from the subroutine `stpnt`, see [2].

5 Examples

To illustrate the algorithms outlined above, we investigate essential and absolute spectra for the complex Ginzburg–Landau and the FitzHugh–Nagumo equation[1].

5.1 The complex Ginzburg–Landau equation

We consider wave trains of the complex Ginzburg–Landau equation (CGL)

$$A_t = (1+\mathrm{i}\alpha)A_{xx} + A - (1+\mathrm{i}\beta)A|A|^2 \tag{5.1}$$

which is an approximate modulation equation valid near the onset of certain instabilities of the essential spectrum [5].

Periodic wave-train solutions of (5.1) are given by $A_* = r\mathrm{e}^{\mathrm{i}(\kappa x-\omega t)}$ with $r^2 = 1-\kappa^2$ and $\omega = \beta + (\alpha-\beta)\kappa^2$. In the detuned variable $A = \tilde{A}\mathrm{e}^{-\mathrm{i}\omega t}$, the equation becomes, upon omitting tildes,

$$A_t = (1+\mathrm{i}\alpha)A_{xx} + (1+\mathrm{i}\omega)A - (1+\mathrm{i}\beta)|A|^2A$$

with solutions $A_* = r\mathrm{e}^{\mathrm{i}\kappa x}$. For the linearization about these wave trains, we consider B and $\bar{B}$ as independent variables, not necessarily complex conjugate, and obtain the linearization

$$\begin{aligned}\lambda B &= (1+\mathrm{i}\alpha)B_{xx} + (1+\mathrm{i}\omega)B - (1+\mathrm{i}\beta)(2|A_*|^2B + A_*^2\bar{B})\\ \lambda\bar{B} &= (1-\mathrm{i}\alpha)\bar{B}_{xx} + (1+\mathrm{i}\omega)\bar{B} - (1-\mathrm{i}\beta)(2|A_*|^2\bar{B} + \bar{A}_*^2B).\end{aligned}$$

Next, we substitute $B = b\mathrm{e}^{\mathrm{i}\kappa x+\nu x}$ and $\bar{B} = \bar{b}\mathrm{e}^{-\mathrm{i}\kappa x+\nu x}$, where we view b and $\bar{b}$ as independent variables. We obtain the analogue to the matrix in (4.10) for the dispersion relation

$$\mathcal{D}(\lambda,\nu) = \begin{pmatrix}(1+\mathrm{i}\alpha)(\nu+\mathrm{i}\kappa)^2 & 0\\ 0 & (1-\mathrm{i}\alpha)(\nu-\mathrm{i}\kappa)^2\end{pmatrix} + a - \lambda\,\mathrm{id}$$

where

$$a = \begin{pmatrix}1+\mathrm{i}\omega-2(1+\mathrm{i}\beta)r^2 & -(1+\mathrm{i}\beta)r^2\\ -(1-\mathrm{i}\beta)r^2 & 1-\mathrm{i}\omega-2(1-\mathrm{i}\beta)r^2\end{pmatrix}$$

which simplifies to

$$\mathcal{D}(\lambda,\nu) = \begin{pmatrix}(1+\mathrm{i}\alpha)(\nu^2+2\mathrm{i}\kappa\nu)-(1+\mathrm{i}\beta)r^2 & -(1+\mathrm{i}\beta)r^2\\ -(1+\mathrm{i}\beta)r^2 & (1-\mathrm{i}\alpha)(\nu^2-2\mathrm{i}\kappa\nu)-(1-\mathrm{i}\beta)r^2\end{pmatrix} - \lambda\,\mathrm{id}\,.$$

Hence, we obtain a constant-coefficient problem with dispersion relation $d(\lambda,\nu) = \det\mathcal{D}(\lambda,\nu) = 0$, and the approach of §3.3 and §4.2 for $N=2$ applies.

The essential spectrum $\{\lambda;\ d(\lambda,\mathrm{i}\gamma)=0,\ \gamma\in\mathbb{R}\}$ consists of the two explicit curves

$$\lambda_\pm(\mathrm{i}\gamma) = -1+\kappa^2-\gamma(2\mathrm{i}\alpha\kappa+\gamma) \pm \sqrt{(\kappa^2-1)^2-\gamma(4\mathrm{i}\beta\kappa^3+2\alpha\beta\gamma+\alpha^2\gamma^3-4\mathrm{i}\kappa(\beta+\alpha\gamma^2)-2\kappa^2(2+\alpha\beta)\gamma)}. \tag{5.2}$$

We note that $\lambda_-(0)=0$, so zero is always in the essential spectrum (see Figure 2 for the shape of the essential spectrum).

Regarding the absolute spectrum, note that the dispersion relation d has four spatial roots ν for each λ, and the Morse index for the absolute spectrum is therefore two. Furthermore, we expect $\binom{4}{2} = 6$ double roots

[1] The AUTO files used for the following computation are available from the authors upon request.

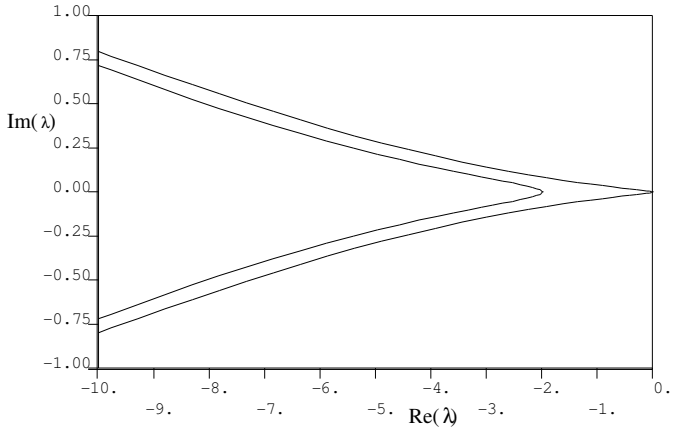

Figure 2: *The essential spectrum of the wave train with wave number* $\kappa = 0.1$ *is plotted for* $(\alpha, \beta) = (0.1, 0.2)$.

by Lemma 4.5; note, however, that this prediction will not hold for $\alpha = 0$ since the diffusion coefficients coincide in this case, and Lemma 4.5 does not apply. Indeed, the resultant of $d(\lambda, \nu)$ and $\partial_\nu d(\lambda, \nu)$ with respect to ν has degree four in that case, hence there are only four double roots (plus two at infinity). We now discuss the set Σ^*_{abs} for various different parameter values.

We focus on the complex Ginzburg–Landau equation, with $\alpha \neq 0$, for which essential and absolute spectrum generally differ. Furthermore, the explicit solution (5.2) is not easy to interpret for general α, β and κ. Therefore, it appears appropriate to use the numerical approaches discussed in §4.2 to compute the absolute spectrum.

Our results are summarized in Figures 3 and 5, where we plot the numerically computed sets Σ^*_{abs} and the indices associated with each segment for three sets of parameter values. The union of the segments with index 2 is the absolute spectrum. Of interest is the onset of absolute instability, which we computed for fixed values of (α, β) as the wave number κ is varied. For $(\alpha, \beta) = (0.1, 0.2)$, the absolute spectrum becomes unstable through a complex conjugate pair of branch points that crosses the imaginary axis, while for $(\alpha, \beta) = (-8, 1)$ all branch points lie to the left of the imaginary axis, and the instability is induced by a curve of absolute spectrum that crosses the imaginary axis.

First, consider $(\alpha, \beta) = (0.1, 0.2)$. Starting with the stable absolute spectrum for $\kappa = 0.1$ shown in Figure 3(i), we continued the branch points in the parameter $\kappa \in [0, 1]$ to locate the onset of absolute instability (see Figure 4). The real stable branch point in the absolute spectrum for $\kappa = 0.1$ shown in Figure 3(i) merges with a branch point of index 3 at $\kappa \approx 0.51$ and $\text{Re}(\lambda) \approx -0.01$. For increasing κ a pair of complex conjugate branch points emerges, each with index 2, and crosses the imaginary axis at $\kappa \approx 0.598$. This is the only crossing of branch points in the absolute spectrum for $(\alpha, \beta) = (0.1, 0.2)$ and $\kappa \in [0, 1]$.

Next, we consider the Ginzburg–Landau equation for $(\alpha, \beta) = (-8, 1)$, which lie in the Benjamin–Feir unstable regime $\alpha\beta < 1$, and focus on the wave train with wave number $\kappa = -0.3$. The generalized absolute spectrum is plotted in Figure 5. In this case, the absolute spectrum is unstable but does *not* contain any branch points. In particular, the instability is a remnant instability (in the terminology of [9]) which cannot be detected by locating branch points of index two.

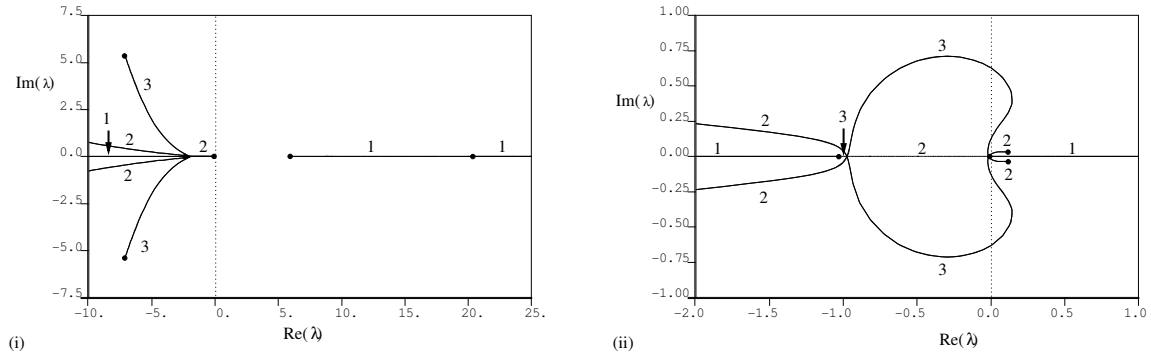

Figure 3: *The absolute spectrum* $\Sigma^*_{\rm abs}$ *is plotted for* $(\alpha,\beta)=(0.1,0.2)$*, where bullets correspond to branch points and numbers indicate the Morse index. (i) For the wave number* $\kappa=0.1$*,* $\Sigma^2_{\rm abs}$ *is stable, and its rightmost point is a branch point at* $\lambda\approx -0.0001$*. (ii) For the wave number* $\kappa=0.7$*,* $\Sigma^2_{\rm abs}$ *is unstable, and its rightmost points are branch points at* $\lambda\approx 0.115\pm 0.036$i *(here we omitted two branch points of index one at* $\lambda\approx 189$ *and* $\lambda\approx 210$*).*

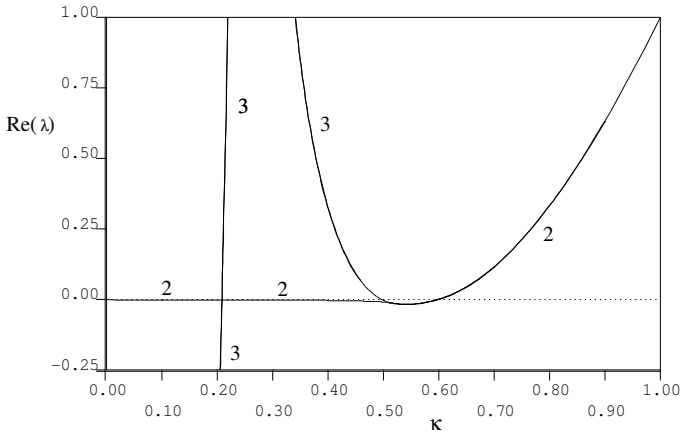

Figure 4: *For* $(\alpha,\beta)=(0.1,0.2)$*, we plot the real parts of branch points with different Morse indices as functions of* κ*. The absolute spectrum* $\Sigma^2_{\rm abs}$ *becomes unstable at* $\kappa\approx 0.598$ *through branch points at* $\lambda\approx \pm 0.032$i *of index two.*

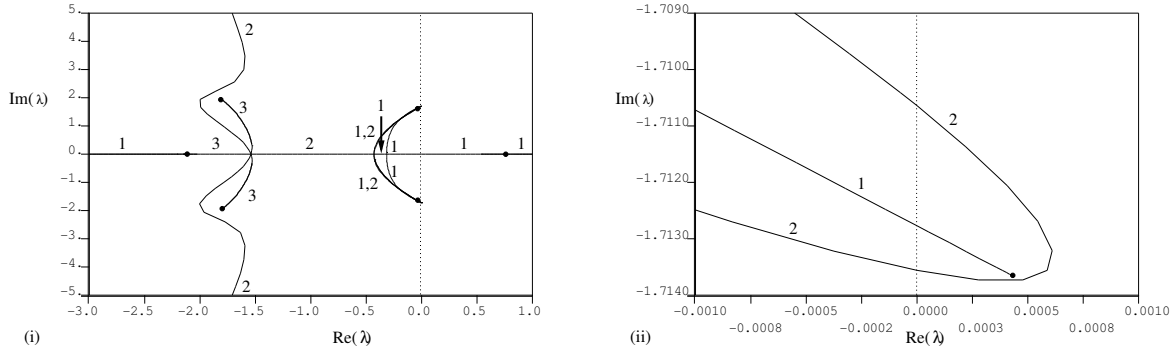

Figure 5: *(i) The absolute spectrum is plotted for* $(\alpha,\beta)=(-8,1)$ *and* $\kappa=-0.3$*. Note that* $\Sigma^2_{\rm abs}$ *is unstable, but that there are no branch points with index two. (ii) Magnification of one of the two symmetric critical regions.*

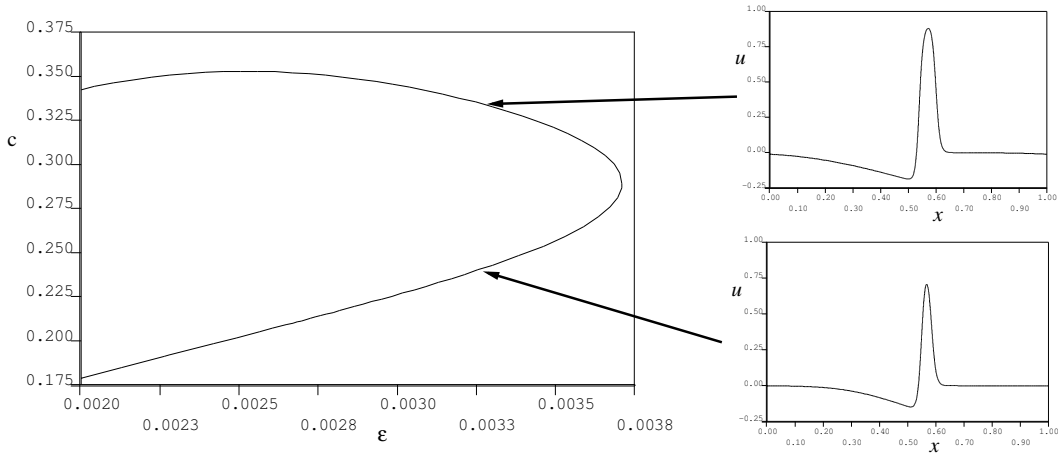

Figure 6: *Bifurcation diagram of wave trains with period* $L = 200$ *to the FitzHugh–Nagumo equation in the* (ϵ, c) *parameter plane. The insets show the* u*-components of the wave-train profiles for* $\epsilon = 0.0033$.

5.2 The FitzHugh–Nagumo equation

We investigate the critical part of the spectrum of wave trains with large spatial period in the FitzHugh–Nagumo equation

$$\begin{aligned} u_t &= u_{xx} + cu_x - v - u(u-1)(u-a) \\ v_t &= \delta v_{xx} + cv_x + \epsilon(u - \gamma v), \end{aligned}$$

written in a comoving frame with speed c.

It is known, from numerical computations and also through some theoretical work, that the FitzHugh–Nagumo equation supports, in an appropriate parameter regime, a fast stable pulse and an unstable slow pulse which disappear in fold or saddle-node bifurcation as the parameter ϵ is increased. Both pulses are accompanied by wave trains with arbitrarily large spatial period, which converge to the pulses as the period is increased, and also undergo saddle-node bifurcations for each fixed period as ϵ is increased. Our objective is to numerically continue the spectrum of these wave trains which will cross through the imaginary axis as we continue the wave trains for a fixed large period through their fold bifurcation. For large periods, the eigenvalues of the pulses generate nearby isola of essential spectrum [3] and so we expect an isola to cross at the fold point. Throughout, we fix the parameters $a = \gamma = 0.2$ and $\delta = 0.25$, and consider the wave trains with spatial period $L = 200$. The bifurcation diagram in (c, ϵ) and the associated solution profiles are shown in Figure 6.

First, to illustrate the PDE spectra near the fold bifurcation, we continue the fast wave trains in the (ϵ, c)-plane until they become the slow wave trains while, at the same time, computing and continuing the simple real eigenvalue of their PDE linearization $\mathcal{L}_0$ that destabilizes the wave train at the fold. The resulting eigenvalue curve is shown in Figure 7.

Next, we compute the entire isolas of essential spectrum that emanate from the fold eigenvalue and from the translation eigenvalue at $\lambda = 0$ for different values of ϵ near the fold bifurcation. As illustrated in Figure 8, the fast wave train destabilizes already before the actually fold bifurcation as the two aforementioned isolas first coalesce at the temporal eigenvalues corresponding to $\nu = \mathrm{i}\pi/L$ to form a single isola, part of which then moves into the right half-plane. Note that the unfolding of the essential spectrum near temporal double root that occurs when the two isolas touch each other is the x-shape crossing that we expect from the list of

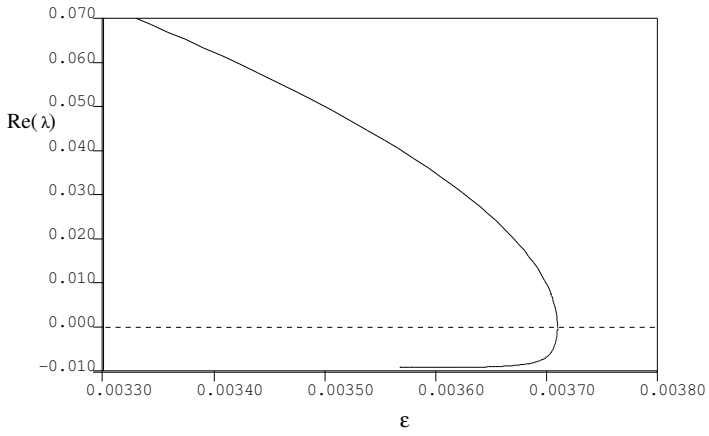

Figure 7: *The real part of the eigenvalue of $\mathcal{L}_0$ that changes sign at the fold bifurcation is plotted as a function of ϵ. Note that the lower branch corresponds to the fast wave trains and the upper one to the slow wave trains.*

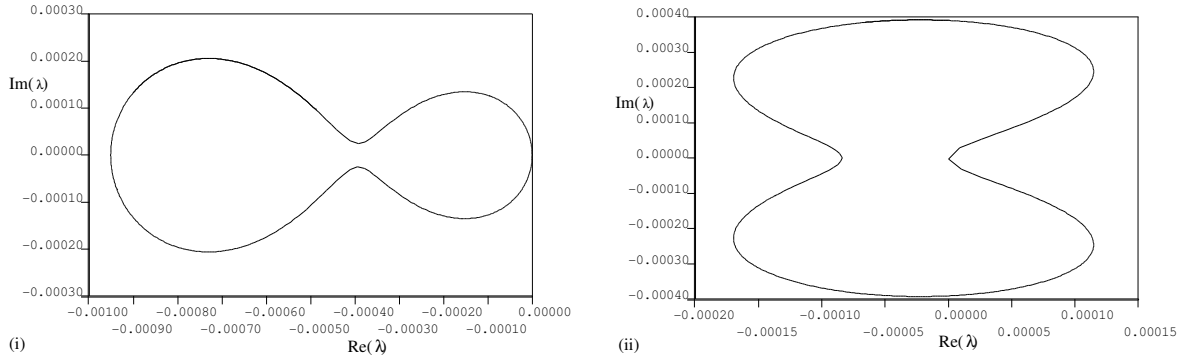

Figure 8: *(i) $\epsilon \approx 0.00371$: The isola corresponding to the fold eigenvalue has merged with the isola at the origin. (ii) $\epsilon \approx 0.00371013$: The merged isolas of the fast wave train before the fold point have already crossed the imaginary axis.*

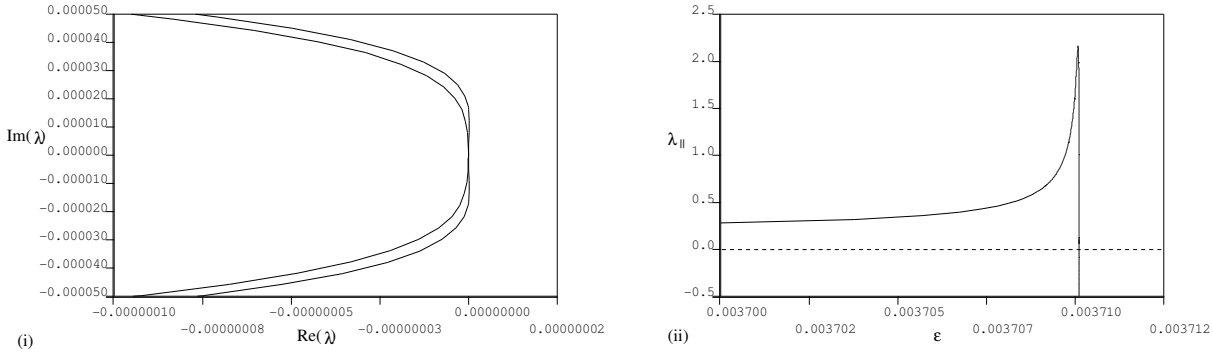

Figure 9: *Details of the onset of instability of the isola shown in Figure 8. (i) We plot an overlay of the critical parts of the isola for $\epsilon \approx 0.00371011259$ and $\epsilon \approx 0.00371011266$. (ii) We plot the tangency coefficient $\lambda_{||}$ (see §3.4.3) as a function of ϵ, which corroborates that the onset occurs at zero wave number.*

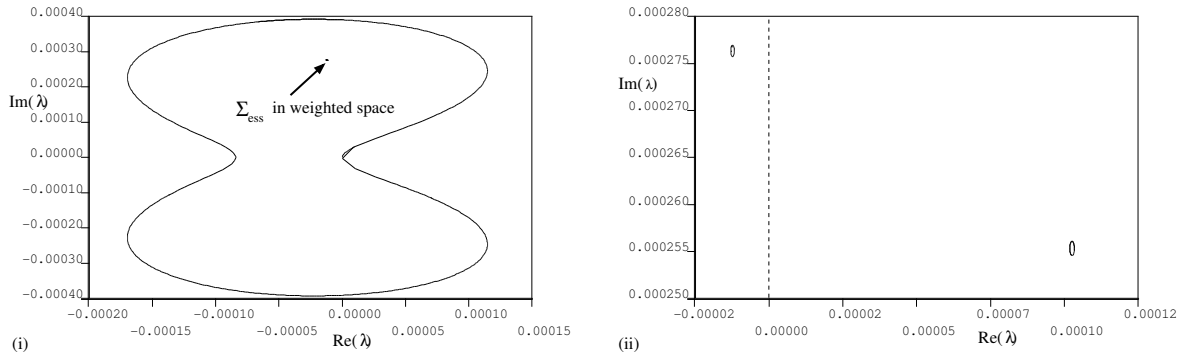

Figure 10: *(i) The isola from Figure 8(ii) in the unweighted space and the upper part of the same isola, now computed in a weighted space with* $\mathrm{Re}\,\nu \approx -0.035$. *(ii) Magnification of the isola in the weighted space for two different values of* ϵ*: the unstable isola to the right corresponds to a value of* ϵ *closer to the fold. Both isolas contain absolute spectrum.*

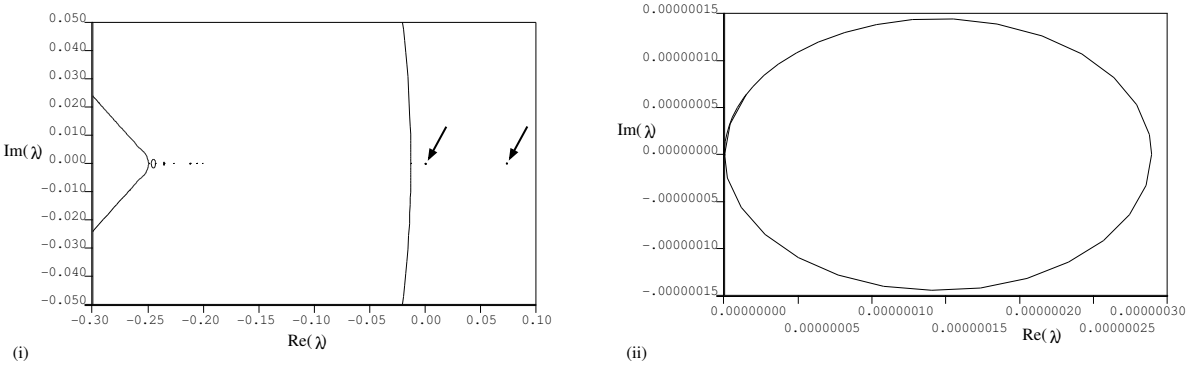

Figure 11: *(i) The essential spectrum of the slow periodic wave train at* $\epsilon = 0.0033$ *near the origin is plotted. The two tiny isola located near* $\lambda = 0$ *and near* $\lambda = 0.08$ *have been enlarged to be visible. (ii) Magnification of the isola which is attached to the origin.*

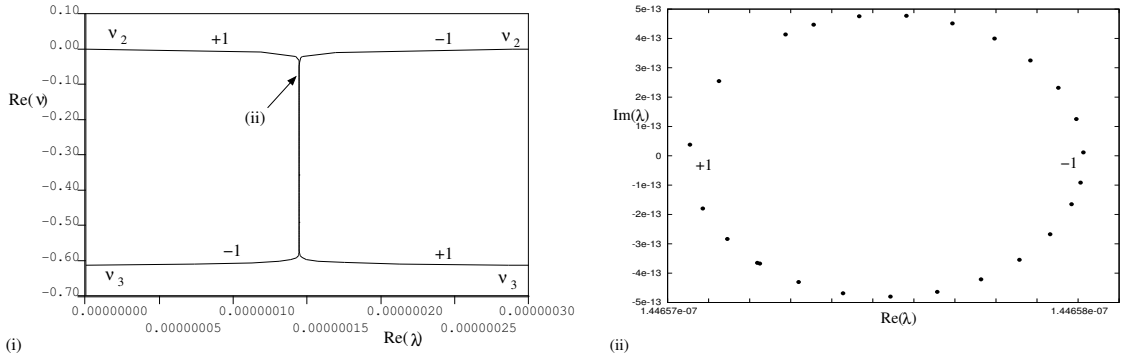

Figure 12: *(i) Real parts of the ordered Floquet exponents ν_2 and ν_3 for $\lambda \in \mathbb{R}$ within the isola of essential spectrum in Figure 11(ii). Here* $\mathrm{sgn}(\mathrm{e}^{\nu_2 L}) = -\mathrm{sgn}(\mathrm{e}^{\nu_3 L})$ *with signs indicated. The crossing point* $\lambda \approx 1.446575 \cdot 10^{-7}$ *lies in the absolute spectrum, which seems hard to continue as a curve. (ii) We plot the isola of essential spectrum in Figure 11(ii) continued to the exponential weight* $\eta \approx -0.075$*, see (i). Signs of real Floquet multipliers are indicated. This isola contains the component of absolute spectrum referred to in (i).*

generic singularities in §3.3.3. Figure 9 indicates that the onset of instability does not occur at finite wave numbers; instead the curvature of the essential spectrum at the origin changes sign, see §3.4.3. We remark that at the fold point the isola has an x-shaped crossing point at the origin and the group velocity changes sign through a singularity.

The merged isola in Figure 8(ii) contains absolute spectrum, which we found hard to compute, however. Instead, we locate it indirectly via isolas of essential spectrum, computed in exponentially weighted spaces, which necessarily contain absolute spectrum of index 2 on account of the discussion in §4.3. Figure 10 shows these isolas inside the isola plotted in Figure 8(ii). The isola containing absolute spectrum moves into the unstable half plane as the parameter ϵ approaches the fold point (see Figure 10(ii)). Thus, the wave train is not only essentially but also absolutely unstable before the fold point.

Lastly, on the branch corresponding to the slow wave train, the merged isolas separate again into an unstable isola which is completely contained in the right half-plane and an isola which emerges from $\lambda = 0$, which is contained in the closed right half-plane (see Figure 11). We computed these spectra using the methods described in §3.4: To locate the two isolas, we used finite differences with 800 grid points and a subsequent direct eigenvalue computation to approximate the spectrum of $\mathcal{L}_0$. The curves attached to the eigenvalues of $\mathcal{L}_0$ are then computed by continuation. Both of these isola contain absolute spectrum, again referring to §4.3. Concerning the isola attached to the origin, we located a point in the absolute spectrum by continuation of two Floquet exponents whose imaginary parts differ by π/L and hence have opposite signs as Floquet multipliers, see Figure 12. The expected curve of absolute spectrum containing this point seems hard to compute. However, since the signs of the real Floquet multipliers e^{ν_2} and e^{ν_3} are opposite, the crossing point of the real parts of the Floquet exponents is not a double root and the attached curve of absolute spectrum should cross the real axis with orthogonal tangent. We remark that this cannot occur for spectra of constant coefficient problems. We bound the location of this curve of absolute spectrum by continuing the isola of essential spectrum in Figure 11(ii) in decreasing exponential weight $\eta = \mathrm{Re}\,\nu \leq 0$. These isola in weighted spaces appear to be concentric circles about the crossing point. We therefore expect that the component of absolute spectrum lies in the smallest isola we computed, a circle of radius $5 \cdot 10^{-13}$, see Figure 12.

Acknowledgments J. Rademacher acknowledges the hospitality at the Free University of Berlin and support from NSF grant DMS-0203301 and from a PIMS fellowship. B. Sandstede acknowledges support from the NSF through grant DMS-0203854 and from a Royal Society/Wolfson research Merit Award. A. Scheel

was partially supported by the NSF through grant DMS-0203301.

References

[1] E. Crampin. *Reaction-diffusion patterns on growing domains*. PhD thesis, University of Oxford, 2000.

[2] E. Doedel, R.C. Paffenroth, A.R. Champneys, T.F. Fairgrieve, Y.A. Kuznetsov, B.E. Oldeman, B. Sandstede, and X. Wang. *AUTO2000: Continuation and bifurcation software for ordinary differential equations (with HOMCONT)*. Technical report, Concordia University, 2002.

[3] Gardner, R.A. *On the structure of the spectra of periodic travelling waves.* J. Math. Pures Appl., IX. **72**, 415–439 (1993)

[4] D. Henry. *Geometric theory of semilinear parabolic equations*. Lecture Notes in Mathematics **840**, Springer, Berlin, 1981.

[5] A. Mielke. The Ginzburg–Landau equation in its role as a modulation equation. In *Handbook of dynamical systems II*, B. Fiedler (ed.), Elsevier 2002. 759-834.

[6] J.D.M. Rademacher. *Homoclinic bifurcation from heteroclinic cycles with periodic orbits and tracefiring of pulses*. PhD Thesis, University of Minnesota, 2004.

[7] J.D.M. Rademacher. Absolute and essential spectra of wave trains. Preprint 2005.

[8] B. Sandstede and A. Scheel. Absolute versus convective instability of spiral waves. *Phys. Rev. E* **62** (2000) 7708–7714.

[9] B. Sandstede and A. Scheel. Absolute and convective instabilities of waves on unbounded and large bounded domains. *Physica D* **145** (2000) 233–277.

[10] B. Sandstede and A. Scheel. On the structure of spectra of modulated travelling waves. *Math. Nachr.* **232** (2001) 39–93.

[11] B. Sandstede and A. Scheel. Gluing unstable fronts and backs together can produce stable pulses. *Nonlinearity* **13** (2000) 1465–1482.

[12] B. Scarpellini. L^2-perturbations of periodic equilibria of reaction-diffusion systems. *Nonl. Differ. Eqns. Appl.* **1** (1994) 281–311.